

# Benzobisoxazole Cruciforms: Heterocyclic Fluorophores with Spatially Separated Frontier Molecular Orbitals

Jaebum Lim,<sup>†</sup> Thomas A. Albright,<sup>†</sup> Benjamin R. Martin,<sup>‡</sup> and Ognjen Š. Miljanic\*,<sup>†</sup>

<sup>†</sup>Department of Chemistry, University of Houston, 136 Fleming Building, Houston, Texas 77204-5003, United States

<sup>‡</sup>Department of Chemistry, Texas State University—San Marcos, 601 University Drive, San Marcos, Texas 78666, United States

## S Supporting Information

**ABSTRACT:** We report the synthesis of nine conjugated cruciform-shaped molecules based on the central benzo[1,2-d:4,5-d']bisoxazole nucleus, at which two conjugated currents intersect at a ~90° angle. Cruciforms' substituents were varied pairwise among the electron-neutral phenyl groups, electron-rich 4-(*N,N*-dimethylamino)phenyl substituents, and electron-poor pyridines. Hybrid density functional theory calculations revealed that the highest occupied molecular orbitals (HOMOs) are localized (24–99%) in all cruciforms, in contrast to the lowest unoccupied molecular orbitals (LUMOs) which are strongly dependent on the substitution and less localized (6–64%). Localization of frontier molecular orbitals (FMOs) along different axes of these cruciforms makes them promising as sensing platforms, since analyte binding to the cruciform should mandate a change in the HOMO–LUMO gap and the resultant optical properties. This prediction was verified using UV-vis absorption and emission spectroscopy: cruciforms' protonation results in hypsochromic and bathochromic shifts consistent with the preferential stabilization of HOMO and LUMO, respectively. In donor–acceptor-substituted systems, a two-step optical response to protonation was observed, wherein an initial bathochromic shift is followed by a hypsochromic one with continued acidification. X-ray diffraction studies of three selected cruciforms revealed the expected ~90° angle between the cruciform's substituents, and crystal packing patterns dominated by [π···π] stacking and edge-to-face [C–H···π] contacts.



## INTRODUCTION

Optical and electronic properties of conjugated π-systems, as well as their reactivity, are profoundly influenced by their frontier molecular orbitals (FMOs).<sup>1</sup> In principle, these important characteristics could be predictably engineered through modulation of molecule's highest occupied (HOMO) and lowest unoccupied (LUMO) molecular orbitals. In reality, the situation is not quite as simple: in most conjugated molecules, FMOs are delocalized and extensively overlap with each other, thus making their independent modification difficult. Recently, several molecular platforms have been designed with spatially separated FMOs which can be autonomously addressed. Among these, a dominant geometric motif is that of *cruciforms*.<sup>2</sup> X-shaped fully conjugated molecules in which two π-circuits intersect at a central core. Some general cruciform structures include tetrakis(arylethynyl)benzenes,<sup>3</sup> distyrylbis(arylethynyl)benzenes,<sup>4</sup> tetrastyrylbenzenes,<sup>5</sup> tetrakisalkynylethenes,<sup>6</sup> and biphenyl-based “swivel”-cruciforms.<sup>7</sup> Not unexpectedly, proposed applications of cruciforms aim to utilize their modular optical and electronic properties, and these systems were suggested as viable fluorescent sensors for a variety of analytes,<sup>3,4,8</sup> organic light-emitters,<sup>9</sup> components of dye-sensitized solar cells,<sup>10</sup> elements for molecular electronics,<sup>7,11,12</sup> and nonlinear optics materials.<sup>3,5</sup>

In all previously studied cruciform systems, the central core of the molecule served as an important, but rather inert, conjugated connector for the two arms of the cruciform.

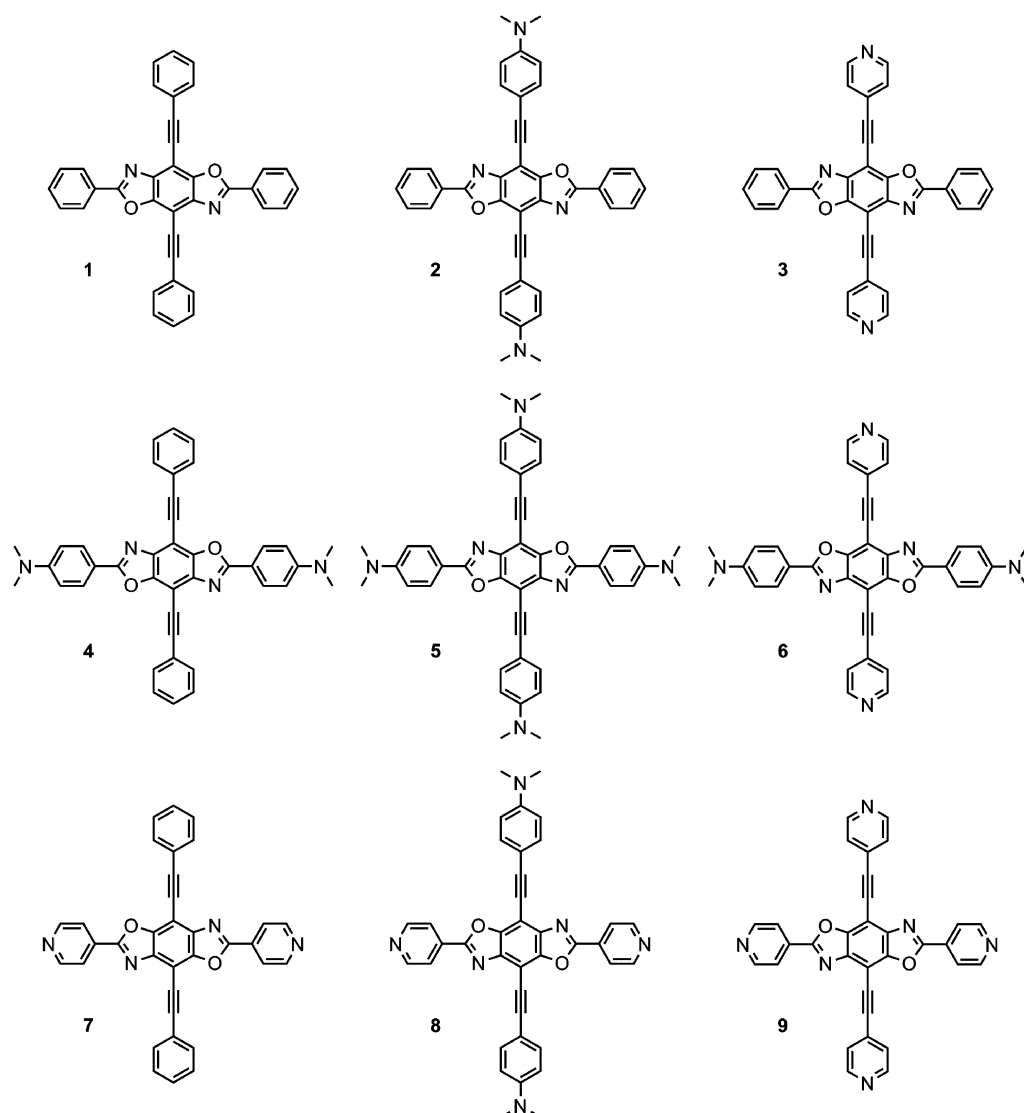
Modification of substituents along these arms was the chief strategy for altering both cruciforms' electronic and molecular recognition properties and relied mostly on the introduction of substituents with resonance and/or inductive donor or acceptor properties. Relatively little attention had been paid to the influence that central core could exert onto the properties of the cruciform. This omission is unusual, as chemical modification of the cruciform's center could dramatically and divergently affect its geometry, bias the electronic properties of the “arms”, and perhaps introduce an additional molecular recognition motif.

Here, we present the synthesis and detailed computational, spectroscopic, and crystallographic investigations of a family of heterocyclic cruciforms with spatially separated FMOs. Fully conjugated cruciform-shaped compounds **1–9** (Chart 1) are characterized by the central heterocyclic benzobisoxazole<sup>13,14</sup> nucleus; emanating from this nucleus are the horizontal benzobisoxazole axis and a vertical bis(arylethynyl)benzene axis. The identity of substituents along each axis was varied from an electron-neutral phenyl group, through an electron-rich 4-(*N,N*-dimethylamino)phenyl substituent, to an electron-poor pyridyl group, with the intention of exploring how electronic effects influence orbital separation and the associated optical characteristics.

Received: October 10, 2011

Published: November 11, 2011

Chart 1. Benzobisoxazole-Based Cruciform-Shaped Compounds Discussed in This Study



Our work was motivated by the pioneering reports of modular synthesis of benzobisoxazole cruciform by Nuckolls and co-workers,<sup>15</sup> who used these systems as components of a molecular electronics toolkit.<sup>16</sup> We have recently demonstrated that benzobisoxazole cruciforms substituted with ester groups form remarkably ordered two-dimensional sheets in the crystal state.<sup>17</sup> In this paper, we present the synthesis of **1–9**, computational investigation of their FMOs, their UV-vis absorption and emission properties, the response of those properties to protonation, and crystal structures of cruciforms **1**, **2**, and **8**.

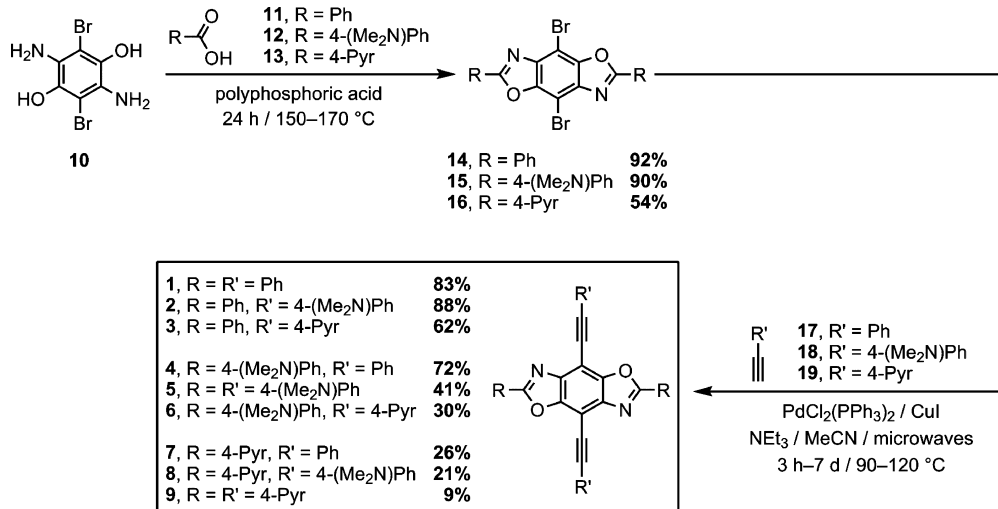
## RESULTS AND DISCUSSION

**Synthesis.** Cruciforms **1–9** were prepared using a variation of our previously reported<sup>17</sup> two-step protocol (Scheme 1). Starting with 2,5-diamino-3,6-dibromobenzene-1,4-diol (**10**),<sup>18</sup> dehydrative condensation with carboxylic acids<sup>19</sup> **11–13** produced sparingly soluble intermediates **14–16**, in which the electronic character of the substituents along the horizontal axis was either neutral (**14**, phenyl), electron-rich (**16**, 4-(dimethylamino)phenyl), or electron-poor (**15**, pyridyl). Each of the three (crude) intermediates was subjected to microwave-

assisted<sup>20</sup> Sonogashira couplings<sup>21</sup> with three different terminal alkynes, phenylacetylene (**17**), 4-ethynyl-N,N-dimethylaniline (**18**), and 4-ethynylpyridine (**19**), to give nine final cruciforms **1–9**. The yields of the final Sonogashira coupling varied from poor to excellent and were probably compromised by (a) low solubilities of starting benzobisoxazoles **14–16**, (b) possible coordination of pyridine-containing cruciforms to the Pd and Cu catalysts,<sup>3e</sup> and (c) electronic mismatch between some alkyne and aryl bromide coupling partners. Pure cruciforms were obtained as yellow to dark red powders following column chromatography and/or crystallization and appear to be stable indefinitely both as solids and in solution. At 25 °C, cruciforms **1–9** are soluble in preparatively useful concentrations in chlorinated solvents, and sparingly, but sufficiently for absorption and emission studies (vide infra), in majority of other common organic solvents.

**Computational Studies.** In order to evaluate the spatial separation of FMOs in cruciforms **1–9** and attempt the prediction of their optical response to acidic analytes, we performed molecular orbital calculations on these systems. Calculations were done using the Gaussian 09W<sup>22</sup> software package and its accompanying graphical interface program

Scheme 1. Synthesis of Cruciforms 1–9



GaussView 5.0. The B3LYP hybrid density functional<sup>23</sup> and a standard 3-21G basis set were used for the geometry optimizations. Compounds **6** and **8** were initially optimized within a  $C_s$  symmetry constraint and both converged to structures with  $C_{2h}$  symmetry. Accordingly, the other cruciform structures were optimized within a  $C_{2h}$  symmetry constraint.

An orbital analysis of the parent bis(ethynyl)benzobisoxazole **20** (Figure 1) revealed that its HOMO is antisymmetric

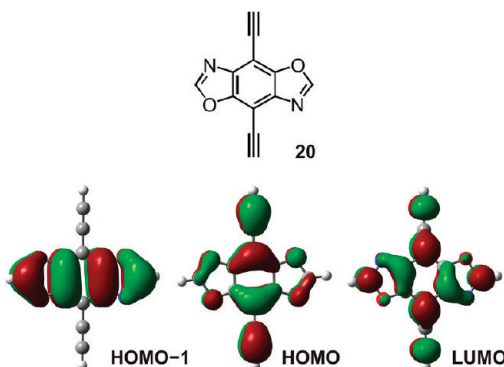


Figure 1. Selected molecular orbitals of the parent bis(ethynyl)benzobisoxazole **20**.

( $b_g$  symmetry in  $C_{2h}$ ) and LUMO symmetric ( $a_u$  symmetry in  $C_{2h}$ ) with respect to the molecule's inversion center. Both orbitals have significant density in the central benzene ring, on the oxazole heteroatoms, and along the  $\text{C}\equiv\text{C}$  bond. The key difference between the two is the orbital density along the oxazole C–H bonds: the HOMO has very little density in that area, but the LUMO does. This means that while both the HOMO and the LUMO can delocalize across the vertical axis of the cruciform, only the LUMO can effectively “spill” over the horizontal axis as well.

This qualitative feature of the parent system translates onto all cruciforms (Figure 2): HOMOs of **1**, **2**, **3**, **5**, **7**, **8**, and **9** have virtually no density in the peripheral rings of the horizontal axis. Significant density in the HOMO along the horizontal axis is found only in cruciforms **4** and **6**, which are both substituted with electron-donating 4-(*N,N*-dimethylamino)phenyl groups. Energetically just below the  $b_g$  HOMO in **20** (0.84 eV lower in

energy) is another orbital of  $b_g$  symmetry (denoted as HOMO–1 in Figure 1). It has very large amplitudes at the oxazole carbons where the horizontal groups are substituted. Therefore, strong electron-donating groups destabilize this orbital so that it becomes the HOMO. In contrast to **4** and **6**, cruciform **5** has four 4-(*N,N*-dimethylamino)phenyl substituents, along both the horizontal and vertical axes, but still localizes its HOMO along the vertical axis since the electron donating substituents destabilize both the HOMO and HOMO–1 by approximately the same amount. Analysis of the LUMO distributions is somewhat more complex, as this orbital communicates freely with both the horizontal and vertical axes of the molecule. The substitution is thus critical in determining whether the LUMO will be localized and, if so, on which portion of the molecule. To put our analysis of orbital localization onto a quantitative footing, we performed a simple numeric analysis of corresponding orbital coefficients. Each cruciform was divided into its horizontal (shaded in light red, illustrated on compound **9** in Figure 2) and vertical (shaded in light blue, illustrated on compound **9** in Figure 2) axis. The atoms of the central benzene ring were ignored because they belong to both axes, and all cruciforms show significant FMO overlap in that region. Then, for both the HOMO and the LUMO, squared orbital coefficients for “vertical” atoms were summed, divided by the sum of squared orbital coefficients for all atoms in the cruciform (excluding the central benzene ring), and multiplied by 100. The resulting number represents the percentage of HOMO/LUMO density along the vertical axis of the molecule (%<sub>v</sub>, Figure 2). The analogous process was repeated for the horizontal axis (%<sub>h</sub>, Figure 2); for each individual orbital, the percentage distributions on the vertical and horizontal axes added up to 100%. The corresponding axis localization percentages are shown next to the individual orbital representations in Figure 2. Finally, each orbitals' localization is described by a single number (Figure 2, numbers in squares) which is defined as localization percentage and is equal to %<sub>h</sub> – %<sub>v</sub>.<sup>24</sup>

Several general trends can be observed. In all cruciforms, the HOMO is more localized than the LUMO, and, regardless of the extent of localization, the HOMO and the LUMO are mostly positioned along different axes of the molecule, except in cruciform **3**. Cruciform **6** has both the most localized HOMO (99%) and the most localized LUMO (64%) and, thus, has the highest spatial separation of FMOs. Also strongly

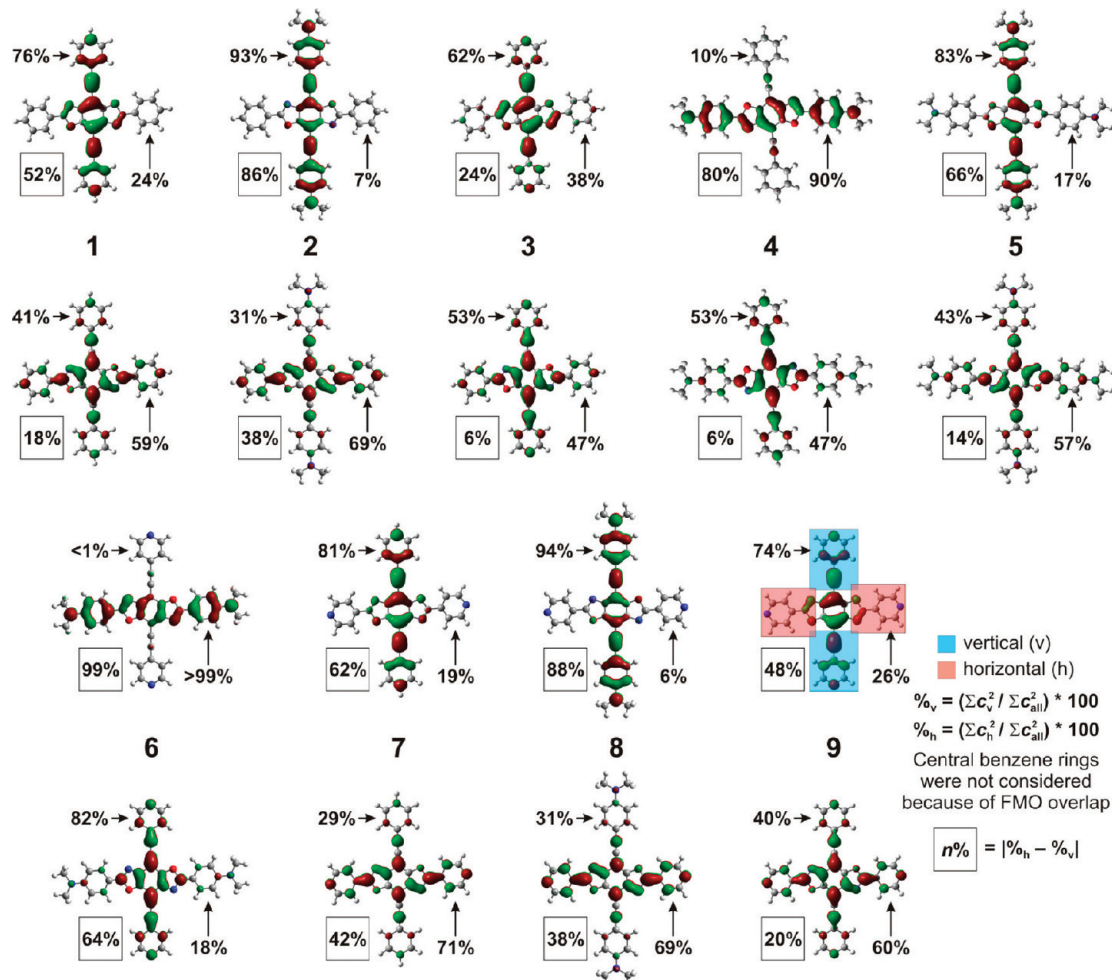


**Figure 2.** FMOs for cruciforms 1–9. HOMOs shown above the corresponding cruciform's number, LUMOs below it. The two percentages next to each orbital's representation denote their relative densities along the vertical ( $\%_v$ ) and horizontal ( $\%_h$ ) axis of the corresponding molecule (for axes definition, see molecule 9). Number in the square next to each orbital's representation indicates that orbital's relative localization (0%, completely delocalized; 100%, completely localized).

separated are the FMOs of 2, 8, and 7 (to a somewhat attenuated degree). Cruciforms 4 and 5 have strongly localized HOMOs (80 and 66%, respectively), but rather delocalized LUMOs (6 and 14%, respectively). Finally, FMOs of cruciforms 1, 3, and 9 are relatively delocalized (6–52% localization). These trends are caused by the combination of (1) predisposition of the bis(ethynyl)benzobisoxazole skeleton to localize its HOMO orbital along the vertical axis, and (2) the donor/acceptor substitution pattern, which tends to localize the HOMO along the electron-richer and the LUMO along the electron-poorer axis of the molecule. The latter factor is general and has precedence in Bunz's<sup>4b,c,j–l,p,q</sup> and Haley's<sup>3a,e,g</sup> systems, but the former effect of the benzobisoxazole core is unique, and it introduces an additional level of control over the orbital separation in cruciform systems.

These computational results suggest what the sensing response of individual cruciforms should be. Cruciforms 2, 6, 7, and 8 would bode well as sensors for protons (and possibly metals), since analyte binding to their basic sites should dominantly affect one of the FMOs and, thus, alter the HOMO–LUMO gap. Protonation of cruciform 2 should occur at its basic dimethylaniline sites; thus, the HOMO should be stabilized, leading to a blue (hypsochromic) shift in absorption (Figure 3). In contrast, cruciform 7 should be protonated along

the horizontal pyridine-bearing axis, leading to a stabilized LUMO and a corresponding red (bathochromic) shift. Donor–acceptor-substituted compounds 6 and 8 present interesting

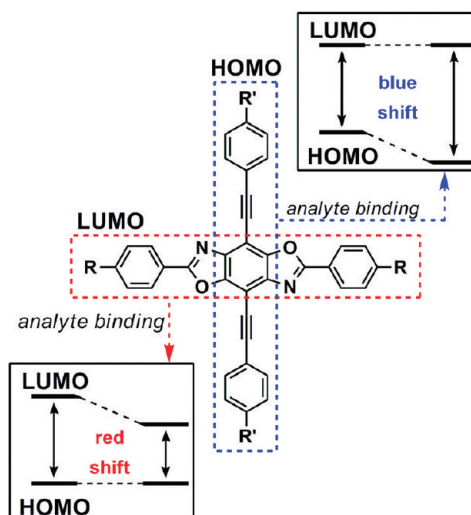


**Figure 3.** Anticipated optical shifts accompanying analyte binding to different portions of cruciforms with spatially separated FMOs.

cases because of their two possible nonequivalent protonation sites. Protonation at their pyridine-based LUMOs would cause a red shift, while protonation along the dimethylaniline-centered HOMO would cause a blue shift. With a sufficient amount of acid, both shifts could occur in a sequence, but it is hard to predict which one would be first: tabulated  $pK_a$  values for parent dimethylaniline and pyridine are virtually identical (5.15 and 5.25, respectively) and can vary by as many as four  $pK_a$  units depending on the substituent in the 4-position.<sup>25</sup> In the next two sections, we will explain how optical spectroscopy was used to establish the order of protonation.

Cruciforms **4** and **5** have only one of their frontier orbitals localized. In **4**, protonation along the horizontal axis should affect both FMOs but would exhibit significantly larger stabilizing effect on HOMO, thus presumably leading to a blue shift analogous to that in **2**. In **5**, basic groups are positioned along both the horizontal and the vertical axes. Protonation of “vertical” nitrogens would lead to a blue shift (stabilized HOMO), while protonation of “horizontal” basic groups should lead to a (smaller) red shift. Again, order of protonation is difficult to predict a priori and had to be elucidated experimentally.

Finally, cruciforms **1**, **3**, and **9** are expected to show uneventful optical response to protonation, as any change would likely affect both the HOMO and the LUMO to a comparable extent.

Computations also produced HOMO–LUMO energy gap values (Table 1), which roughly correlate with  $\lambda_{\max}$  values obtained from UV/vis spectra (vide infra).

**Table 1. Optical Properties and Calculated HOMO–LUMO Gaps for Cruciforms 1–9**

compd	absorption $\lambda_{\max}$ (nm)	emission $\lambda_{\max}$ (nm)	Stokes shift (cm <sup>-1</sup> )	calcd HOMO–LUMO gap (eV, nm)
<b>1</b>	367	407	2678	3.16, 392
<b>2</b>	443	529	3670	2.47, 502
<b>3</b>	368	419	3308	3.24, 383
<b>4</b>	437	497	2763	2.98, 416
<b>5</b>	421	486	3177	2.87, 432
<b>6</b>	458	544	3452	2.79, 444
<b>7</b>	367	439	4469	3.01, 412
<b>8</b>	468	597	4617	2.44, 508
<b>9</b>	367	409	2798	3.17, 391

**Optical Properties.** Dilute solutions of cruciforms **2**, **4**–**6**, and **8** are strongly colored (Figure 4A). Under a hand-held UV

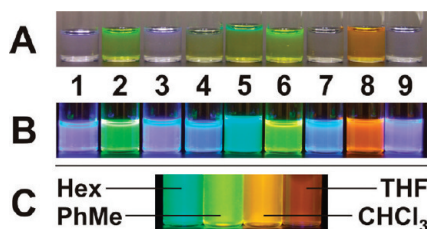


**Figure 4.** (A) Colors of  $\text{CH}_2\text{Cl}_2$  solutions of cruciforms **1**–**9** under visible light. (B) Fluorescence colors of  $\text{CH}_2\text{Cl}_2$  solutions of **1**–**9** under light from a hand-held UV lamp ( $\lambda_{\text{exc}} = 365$  nm). (C) Strong fluorescence solvatochromic behavior of **8** ( $\lambda_{\text{exc}} = 365$  nm).

lamp ( $\lambda_{\text{exc}} = 365$  nm), all of the prepared cruciforms also exhibit bright emission (Figure 4B). Emission wavelengths of

donor–acceptor systems (e.g., **8**, Figure 4C) also show a strong solvent dependence, suggesting a charge-separated excited state.<sup>3d,e,4p</sup>

All prepared cruciforms were analyzed by UV/vis absorption and emission spectroscopies in dilute  $\text{CH}_2\text{Cl}_2$  solutions. Their normalized absorption and emission spectra are shown in Figure 5, grouped into three sets of three spectra each, that correspond to cruciforms with an identical horizontal axis. In general, electronic absorption spectra of cruciforms **1**–**9** are characterized by two broad bands: the lower energy band appearing between approximately 350 and 500 nm and the higher energy absorption between approximately 300 and 400 nm. UV/vis spectra of **1** and **3** are almost superimposable; in contrast, the lowest energy absorption of **2** is bathochromically shifted by 75 nm, indicating possible intramolecular charge transfer (Figure 5, left).<sup>3d,e,4p</sup> The orbital pictures are consistent with this explanation. The FMOs of **2** are spatially significantly more separated than the delocalized FMOs of **1** and **3**. This situation also occurs in the spectra of **7**–**9** (Figure 5, right). The absorption spectra of **7** and **9** are almost superimposable, but in their emission spectra,  $\lambda_{\max}$  for **7** is slightly bathochromically shifted, consistent with a greater degree of donor–acceptor character (relative to **9**). A 100 nm shift to lower energies in the spectrum of **8** (with spatially separated orbitals) is indicative of charge-transfer. In compounds **4**–**6**, qualitative differences in UV/vis spectra are the largest, but their  $\lambda_{\max}$  values are quite similar, in the 430–457 nm range. As is expected, compound **6** with significantly separated FMOs and presumably the strongest charge-transfer, has the highest  $\lambda_{\max}$  among the three. The normalized emission spectra (Figure 5) parallel these observations very closely.

**Optical Response to Protonation.** Since cruciforms **1**–**9** carry basic pyridyl, 4-(*N,N*-dimethylamino)phenyl, and oxazole groups, our next series of experiments examined their optical (UV/vis absorption and emission) response to protonation with trifluoroacetic acid (TFA). All of these experiments were performed in dilute  $\text{CH}_2\text{Cl}_2$  solutions and their results have been summarized in Figure 6 for absorption spectra and Figure 7 for emission spectra. As predicted by the orbital analysis, the absorption spectra of cruciforms with poorly localized FMOs, **1**, **3**, and **9** showed negligible response to protonation. However, the changes in their emission spectra were more dramatic. Compound **1** showed the quenching of fluorescence at high TFA concentrations, which we tentatively attribute to the eventual protonation of oxazole nitrogen atoms. In the emission spectra of compounds **3** and **9**, a significant red shift was observed around  $-\log[\text{TFA}]$  of 3.71, consistent with pyridine protonation.<sup>26</sup>

The spectra of cruciforms **4** and **5**, which have partially separated FMOs, are quite diagnostic. Protonation of **4** causes a pronounced blue shift in both absorption and emission spectra, consistent with stabilization of its HOMO. In **5**, a slight red shift in both absorption and emission, most apparent at  $-\log[\text{TFA}] = 2.31$ , is followed by a more pronounced blue shift with continued acidification. Such behavior is consistent with initial protonation along the horizontal dimethylamino groups, which should stabilize the LUMO, and secondary protonation along the vertical axis, which should strongly stabilize the more localized HOMO.

Cruciform **2**, with its strongly separated FMOs, is protonated at its dimethylamino groups positioned along the vertical axis. Upon protonation, stabilization of the HOMO is apparent from blue shifts in both absorption and emission spectra. As in **1**, the

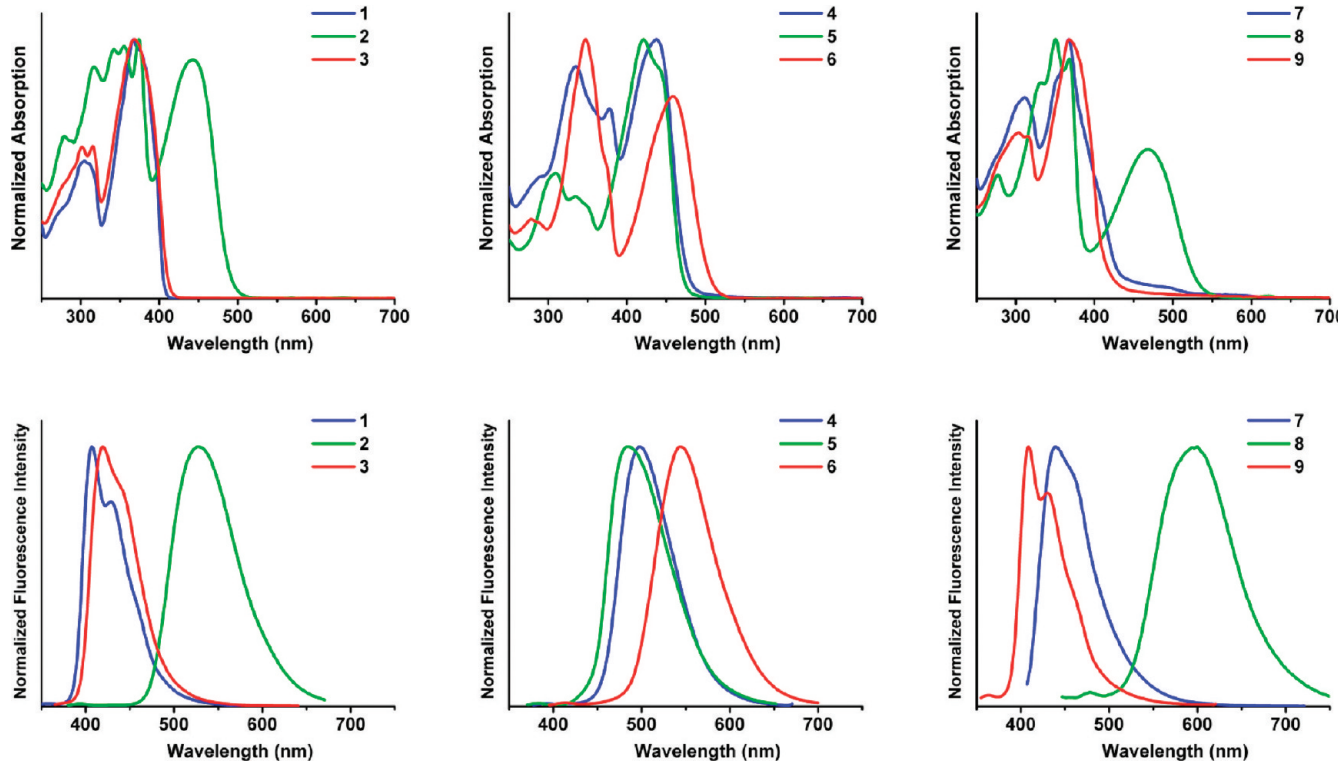


**Figure 5.** Normalized UV-vis absorption (top) and emission (bottom) spectra of benzobisoxazole cruciforms **1–9** in  $\text{CH}_2\text{Cl}_2$ . Excitation wavelengths used were 320 (**1**), 350 (**2** and **4**), 335 (**3**), 341 (**5**), 356 (**6**), 377 (**7**), 417 (**8**), and 325 (**9**) nm.

blue-shifted emission is partially quenched in very acidic solutions, which we attribute to partial protonation of the oxazole rings. Cruciform **7** exhibits a rather moderate red shift in absorption and quenching of fluorescence upon protonation; the former effect is consistent with dominant protonation along its LUMO-bearing horizontal axis, but is puzzlingly unpronounced—given the strong spatial separation of calculated FMOs. Together with the results on protonation of **5**, this observation would suggest that both pyridyl and dimethylamino groups are more basic when positioned along the cruciforms' horizontal axes. This effect is probably caused by the influence of the HOMO–1 orbital which donates electron density to the substituents positioned along the horizontal axes, and is especially relevant in the case of electron-donating 4-(*N,N*-dimethylamino)phenyl substituents.

Finally, spectra of donor–acceptor cruciforms **6** and **8** reveal a distinct two-step optical response to protonation. Initially, protonation causes a red shift in absorption spectra of both compounds, most pronounced at  $-\log[\text{TFA}] = 3.01$ . Quenching of emission from both compounds suggests that the initial protonated species is nonfluorescent. The red shift is explained by the initial protonation of the pyridine nitrogen atoms in both cruciforms, regardless of their positioning on horizontal or vertical axis. These results stand in contrast to those of Bunz<sup>41</sup> and Haley,<sup>3e</sup> who observed that *N,N*-dibutylanilines protonate before pyridines. This difference may be caused by the stronger stabilization of protonated pyridines through conjugation with the 4-substituent (vs protonated anilines).<sup>27</sup> With continued acidification both **6** and **8** recover their fluorescence, which is now blue-shifted. Absorption maxima are also blue-shifted, indicative of a second protonation along the electron-rich HOMO-bearing axis.

All observed protonation-induced optical changes could be fully reversed by addition of a base such as  $\text{NEt}_3$ .

**Crystallographic Studies.** Before this study, there were only three reported crystal structures of benzo[1,2-*d*:4,5-*d'*]-bisoxazoles: one published by Nuckolls,<sup>15a</sup> and two from our previous work.<sup>17,28</sup> We deemed crystallographic investigations of compounds **1–9** interesting as their regular geometries and highly localized FMOs could lead to the formation of donor–acceptor stacks in the solid state. All prepared cruciforms are solids, but obtaining single crystals of sufficiently high quality for X-ray diffraction proved challenging. After extensive experimentation, we were able to grow single crystals of cruciforms **1** and **2** by slowly diffusing hexane into their solutions in  $\text{CHCl}_3$ , and those of cruciform **8** by slowly diffusing hexane into its  $\text{CH}_2\text{Cl}_2$  solution.<sup>15a,29</sup>

Cruciform **1** crystallizes in the  $R\bar{3}$  space group with nine molecules of **1** in the unit cell. The molecules of **1** are organized into stacks which are tilted relative to the crystallographic *c*-axis. Six of these stacks (which alternate in their tilting orientation) surround each 3-fold rotation axis. While the atoms comprising the molecules of **1** could be modeled without disorder, numerous electron density peaks (presumably due to disordered molecules of  $\text{CHCl}_3$ ) were found along the rotation axes, lying in the tunnels generated by the stacked molecules. As these peaks could not be rigorously modeled, we used the PLATON/SQUEEZE routine<sup>30</sup> to subtract the delocalized electron density from the structure. The equivalent of 33 electrons/unit cell were identified by the routine (corresponding to approximately 0.6 molecules of  $\text{CHCl}_3$  per unit cell). The crystal structure of **1** (Figure 8A) reveals an essentially planar molecule, with minimal distortions of peripheral phenyl rings relative to the average plane of the benzobisoxazole nucleus. The phenyl rings oriented along the

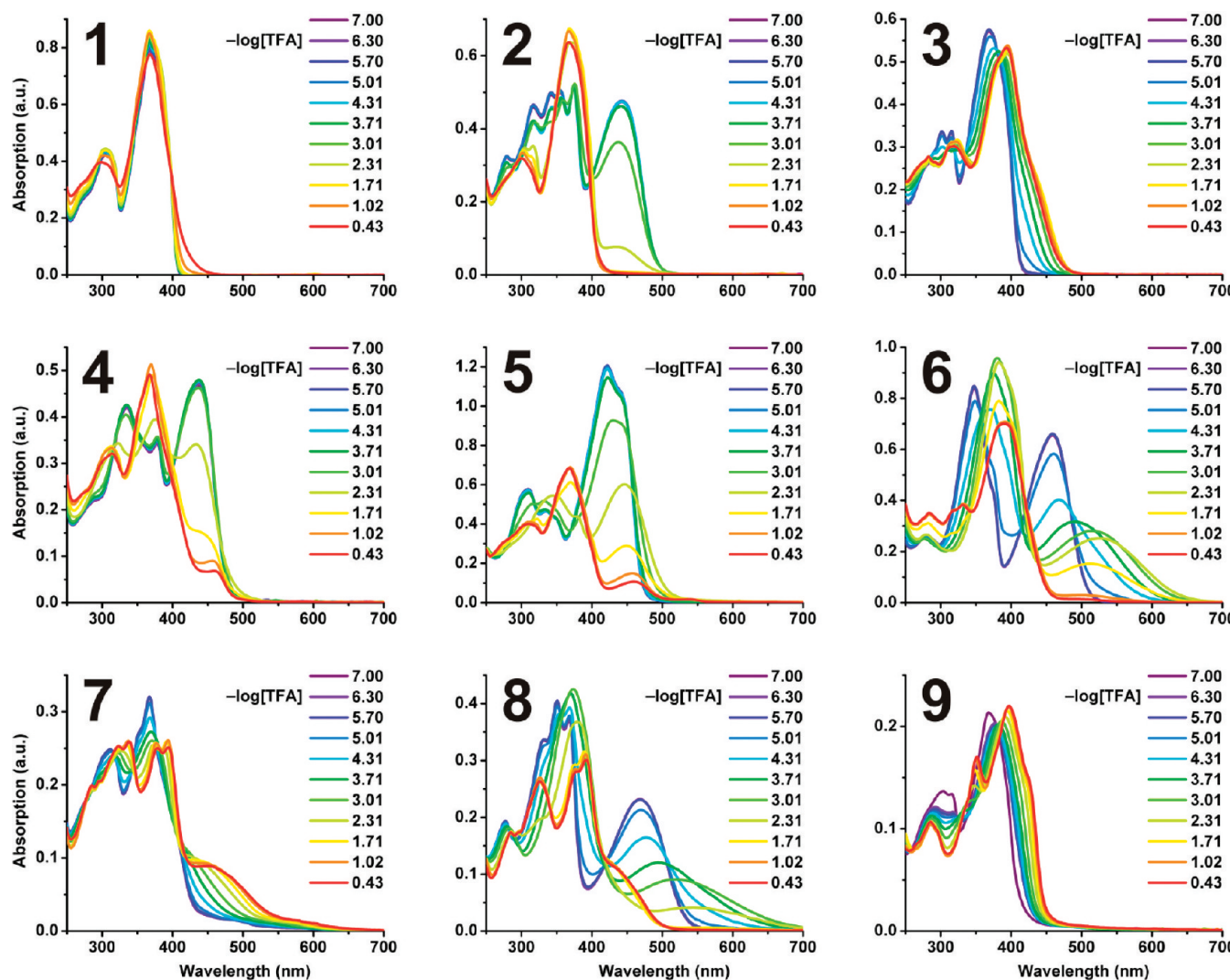


**Figure 6.** Changes in the UV-vis absorption spectra of benzobisoxazole cruciforms **1–9** in  $\text{CH}_2\text{Cl}_2$  in response to protonation with trifluoroacetic acid (TFA).

horizontal plane are at a  $5.7^\circ$  angle relative to the central plane, while the “vertical” phenyl rings define a  $5.9^\circ$  angle with the molecule’s center. As expected, the four valences on the benzobisoxazole nucleus define angles<sup>31</sup> very close to ideal  $90^\circ$ —alternating between  $88.1$  and  $91.9^\circ$ . The triple bonds of **1** are essentially undeformed, with  $\text{C}\equiv\text{C}-\text{C}$  angles of  $178.9$  and  $179.6^\circ$ . Molecules of **1** stack in an offset arrangement with average interplanar distances of  $3.44 \text{ \AA}$ , consistent with  $[\pi\cdots\pi]$  interactions.<sup>32</sup> Within each molecule, hydrogen in the para-position of the “horizontal” phenyl rings also establishes short ( $2.58 \text{ \AA}$ )<sup>33</sup> contacts with the nitrogen of the benzobisoxazole nucleus in the neighboring set of stacked molecules. The interdigitated stacks with short  $[\text{C}-\text{H}\cdots\pi]$  contacts in the overall structure parallel those observed by Nuckolls.<sup>15a</sup>

Cruciform **2** crystallizes in the  $\text{C}2/c$  space group, with four molecules of **2** in the unit cell. As in the structure of **1**, significant disorder of the solvent molecules ( $\text{CHCl}_3$ , located in disk-shaped cavities) was treated using the PLATON/SQUEEZE routine (134 electrons were identified, equivalent to an average of 2.3 molecules of disordered  $\text{CHCl}_3$  per unit cell).<sup>30</sup> Its crystal structure (Figure 8B) is notably different from that of **1**: an essentially planar benzobisoxazole axis and almost perpendicular positioning of the substituents along the

bisethynylbenzene axis, with an  $82.6^\circ$  angle between the two planes. The angles between the four valences of the benzobisoxazole alternate between  $89.2$  and  $90.8^\circ$ , with negligible deformations in the  $\text{C}\equiv\text{C}$  bonds ( $179.3$  and  $179.6^\circ$ ). The difference in molecular structures between **1** (essentially coplanar) and **2** (divided between two perpendicular planes) is translated into different supramolecular organizations for the two cruciforms. Thus, while offset face-to-face  $[\pi\cdots\pi]$  contacts dominate the crystal structure of **1**, molecules of **2** associate primarily through three distinct sets of  $[\text{C}-\text{H}\cdots\pi]$  interactions<sup>34</sup> established between (1) the hydrogens on the vertical 4-(*N,N*-dimethylamino)phenyl rings of one molecule and the central benzobisoxazole  $\pi$ -system of another ( $2.48 \text{ \AA}$ ), (2) hydrogens in the para-position of the “horizontal” phenyl rings of one molecule and the  $\text{C}\equiv\text{C}$  bond of another ( $2.86 \text{ \AA}$ ), and (3) hydrogens in the meta- and ortho-positions of the “horizontal” phenyl rings of one molecule and the horizontal phenyl rings of adjacent molecules ( $2.82 \text{ \AA}$ ).<sup>33</sup> Face-to-face stacking is evident only in the  $3.65 \text{ \AA}$  distance between the peripheral 4-(*N,N*-dimethylamino)phenyl rings on adjacent molecules.

Finally, the donor–acceptor cruciform **8** crystallizes in the  $\text{C}2/c$  space group, with four molecules of **8** in the unit cell, and

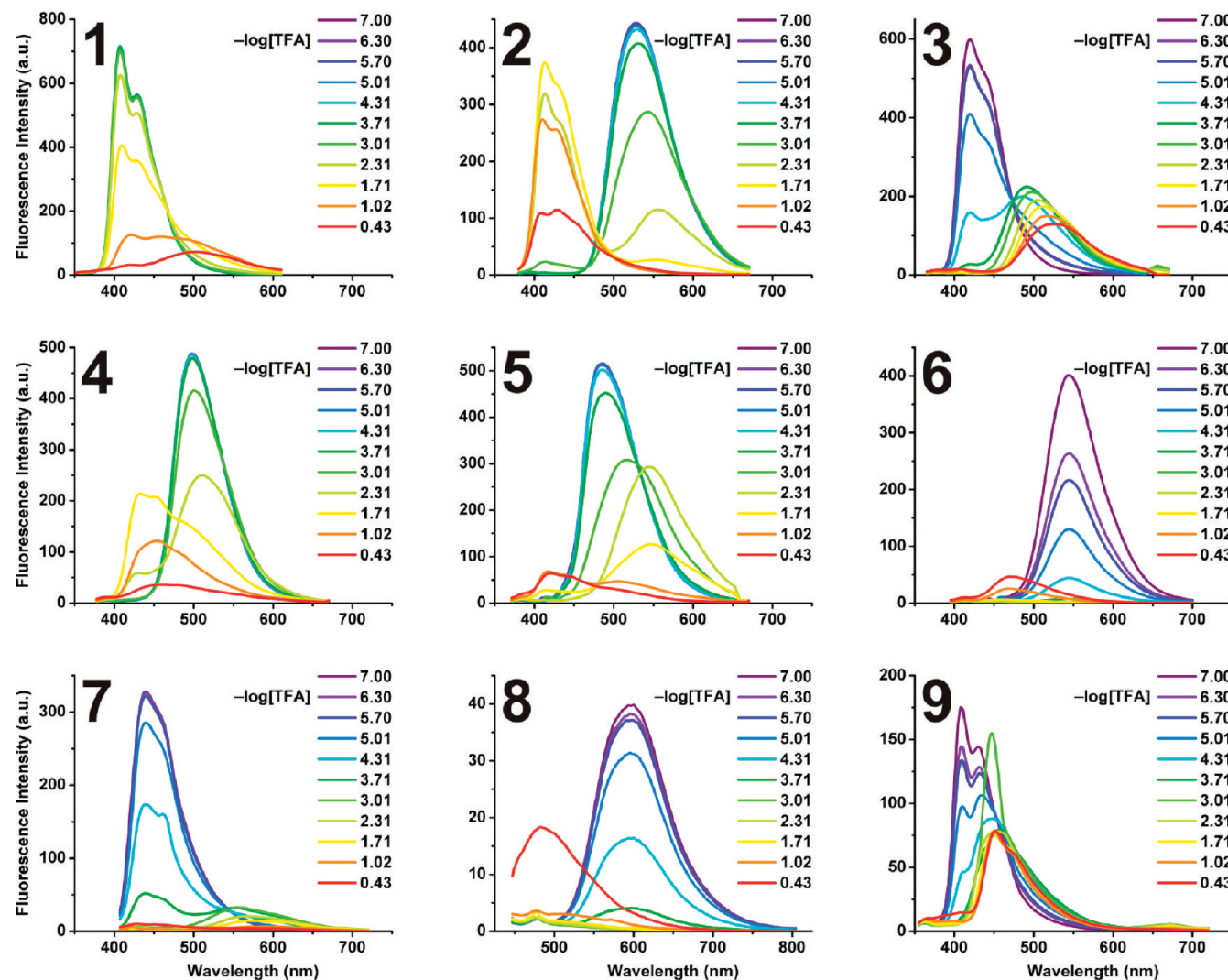


**Figure 7.** Changes in the UV-vis emission spectra of benzobisoxazole cruciforms **1–9** in  $\text{CH}_2\text{Cl}_2$  in response to protonation with trifluoroacetic acid (TFA). Excitation wavelengths used were 320 (**1**), 350 (**2** and **4**), 335 (**3**), 341 (**5**), 356 (**6**), 377 (**7**), 417 (**8**), and 325 (**9**) nm. Note that the wavelength axis of the spectrum of **8** is shifted relative to those of other cruciforms.

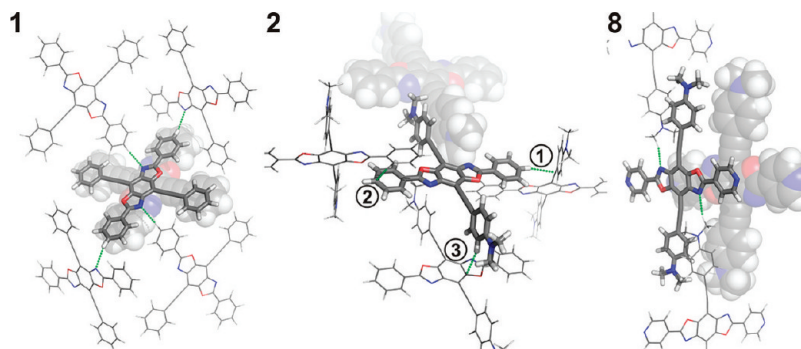


**Figure 8.** Segments of crystal structures of cruciforms **1** (left), **2** (center), and **8** (right). Solvent molecules removed for clarity. Molecules represented by faded space-filling models indicate  $[\pi \cdots \pi]$  stacking relationships, while wireframe models indicate individual short and  $[\text{C}–\text{H} \cdots \pi]$  contacts (contacts are designated by dashed green lines). In the structure of **1**, all four short contacts are identical— $2.58 \text{ \AA}$ ; for **2**, contact 1 is  $2.70 \text{ \AA}$ , contact 2 is  $2.90 \text{ \AA}$ , and contact 3 is  $2.61 \text{ \AA}$ ; for **3**, both indicated short contacts are identical and  $2.65 \text{ \AA}$  long.

one (ordered) molecule of  $\text{CH}_2\text{Cl}_2$  for each molecule of **8**. Analogously to **1**, cruciform **8** (Figure 8C) is essentially planar in the solid state: pyridyl rings are at a  $3.5^\circ$  angle relative to the benzobisoxazole ring plane, while the electron-rich 4-(dimethylamino)phenyl rings define a  $9.4^\circ$  angle with the

benzobisoxazole core. While still highly symmetric, cruciform **8** is the most deformed of the three: angles between benzoxazole valences vary between  $86.9$  and  $93.1^\circ$ , while the triple bonds deform to  $\text{C}\equiv\text{C}$ – $\text{C}$  angles of  $173.1$  and  $178.6^\circ$ . Slipped  $[\pi \cdots \pi]$  stacks are apparent (interplanar distance  $3.32 \text{ \AA}$ ) and

characterized by the positioning of the pyridine rings over benzobisoxazole nuclei (and vice versa). Within the overall structure, interdigitated stacking is observed along the *b* axis, with short contacts established between the hydrogen atoms of the methyl groups in one molecule of **8** and the benzobisoxazole's nitrogen atoms in another (2.65 Å).

Interestingly, none of the three cruciforms crystallographically characterized here resembles the all-parallel organization of carbonyl- and cyano-substituted benzobisoxazole cruciforms previously observed.<sup>17</sup> Also, and somewhat surprisingly, no significant donor–acceptor interactions were noticeable in the crystal structures of either **2** or **8**, despite strong computational evidence supporting spatial separation of their FMOs. Together with our previous results, these three crystal structures suggest that there is no general packing pattern characterizing benzobisoxazole cruciforms. As highly geometrically regular molecules, cruciforms **1**, **2**, and **8** unsurprisingly form closely packed structures—they simply “fit” well together. However, the specifics of the supramolecular structural organization are highly sensitive to the presence of individual functional groups and details of the molecular geometry. Additional details regarding crystallographic characterization can be found in the Supporting Information.

## CONCLUSION

In summary, we have synthesized and exhaustively characterized a family of benzobisoxazole-based cruciform-shaped conjugated molecules. These materials are characterized by modular FMOs, which can be localized onto different portions of the molecule by design. While this behavior parallels that observed previously in Bunz's distyrylbis(arylethynyl)benzenes and Haley's tetrakis(arylethynyl) benzenes, benzobisoxazole cruciforms have at least three additional features that warrant their further study. The horizontal and vertical axes of these cruciforms are electronically quite different, and their arrangement enforces a certain degree of frontier orbital separation that is independent of substitution. This “inherent” FMO separation in **1–9** is quite moderate, and intervention of substituents is still needed to produce systems with highly localized HOMOs and LUMOs. The rigid geometry of benzobisoxazole cruciforms is characterized by the 90° angle between the four benzobisoxazole valences, which is a rather unique arrangement in organic chemistry. This highly regular structure should facilitate their incorporation into solid-state extended structures with crystallographic order. Finally, the heterocyclic central benzobisoxazole core could act as more than just an “innocent bystander”—in contrast to the benzene center of previously described systems—serving perhaps as an additional recognition motif.

Our results open several avenues of future investigation. Synthetically, incorporation of different donor and acceptor groups, as well as modification of their arrangement around cruciforms' axes would be of interest.<sup>3d,e</sup> In addition, more sophisticated functionalities could be included in the structures of these molecules to render their molecular recognition properties specific for individual cationic, anionic, and neutral analytes. Cruciforms **1–9** are potentially appealing as materials with nonlinear optical properties.<sup>35</sup> Finally, integration of geometrically regular benzobisoxazole cruciforms into robust crystalline structures could pave the way for their use as practical solid-state sensors. On a conceptual note, other substructures could be designed as central cores of future molecular cruciforms that would exhibit even larger inherent

separation of FMOs, perhaps entirely independent of substitution. We are actively pursuing several of these directions and the results of these studies will be reported in due course.

## EXPERIMENTAL SECTION

**General Experimental Methods.** Reagents and solvents were purchased from commercial suppliers and used without further purification. Compounds PdCl<sub>2</sub>(PPh<sub>3</sub>)<sub>2</sub><sup>36</sup> and 2,5-diamino-3,6-dibromo-4-hydroquinone (**10**)<sup>18a</sup> were prepared according to literature procedures. Microwave-assisted reactions were performed in a Biotage Initiator 2.0 microwave reactor, producing monochromatic microwave radiation with the frequency of 2.45 GHz. NMR spectra were obtained on spectrometers with working frequencies for <sup>1</sup>H nuclei of 400 and 500 MHz. All <sup>13</sup>C NMR spectra were recorded with simultaneous decoupling of <sup>1</sup>H nuclei. <sup>1</sup>H NMR chemical shifts are reported in ppm units relative to the residual signal of the solvent (CDCl<sub>3</sub>, 7.26 ppm; DMSO-d<sub>6</sub>, 2.50 ppm; THF-d<sub>8</sub>, 1.73 ppm). All NMR spectra were recorded at 25 °C. Column chromatography was carried out on silica gel 60, 32–63 mesh. Analytical TLC was performed on aluminum-backed silica gel plates.

**Synthesis of 2,6-Diphenyl-4,8-dibromobenzo[1,2-*d*;4,5-*d'*]bisoxazole (14).** Benzoic acid (**11**, 902 mg, 7.38 mmol) and compound **10** (1.00 g, 3.36 mmol) were mixed with polyphosphoric acid (14.0 g) in a 100 mL round-bottom flask equipped with a Friedrich condenser. The mixture was heated at 150 °C for 25 h and was then cooled, neutralized with aqueous 1 M NaOH solution, and filtered. The dark solid was washed with H<sub>2</sub>O, EtOH, and then Et<sub>2</sub>O. The solid was air-dried to give 1.45 g (92%, 3.08 mmol) of crude **14** (mp >350 °C, with decomposition). Because of its extremely low solubility, this material was only partially characterized and then used without further purification. **14**. IR (neat): 1608 (w), 1564 (m, ν<sub>O-C≡N</sub>), 1490 (w), 1453 (w), 1319 (m), 1223 (m), 1054 (m), 1025 (m), 974 (m), 912 (m), 873 (m), 773 (m), 719 (m), 693 (s), 683 (s) cm<sup>-1</sup>. <sup>1</sup>H NMR (CDCl<sub>3</sub>, 500 MHz): δ 8.37 (m, 4H), 7.58 (m, 6H). <sup>13</sup>C NMR (CDCl<sub>3</sub>, 125 MHz): δ 164.8, 147.2, 139.9, 132.6, 129.3, 128.4, 126.4, 92.1. HRMS (ESI/[M + H]<sup>+</sup>): calcd for C<sub>20</sub>H<sub>11</sub>Br<sub>2</sub>N<sub>2</sub>O<sub>2</sub> 468.9187, found 468.9181.

**Synthesis of 2,6-Bis[*p*-(*N,N*-dimethylamino)phenyl]-4,8-dibromobenzo[1,2-*d*;4,5-*d'*]bisoxazole (15).** In a 100 mL round-bottom flask equipped with a Friedrich condenser, compound **10** (1.00 g, 3.36 mmol) and 4-(*N,N*-dimethylamino)benzoic acid (**12**, 1.22 g, 7.38 mmol) were mixed with polyphosphoric acid (14.0 g) and stirred for 24 h at 160 °C. The mixture was then cooled, neutralized with aqueous 1 M NaOH solution, and filtered. The dark solid was washed with H<sub>2</sub>O, EtOH, and then Et<sub>2</sub>O. After air-drying, the solid was dissolved in 200 mL of a CH<sub>2</sub>Cl<sub>2</sub>/MeOH mixture (9:1) and then passed through a short silica gel column. The solvent was removed in vacuo to give 1.68 g (90%, 3.02 mmol) of **15** (mp >350 °C, with decomposition). **15**. IR (neat): 1612 (s), 1514 (s, ν<sub>O-C≡N</sub>), 1372 (m), 1316 (m), 1224 (m), 1185 (s), 1055 (m), 904 (m), 870 (m), 812 (m) cm<sup>-1</sup>. <sup>1</sup>H NMR (CDCl<sub>3</sub>, 400 MHz): δ 8.19 (d, <sup>3</sup>J<sub>H-H</sub> = 9.16 Hz, 4H), 6.77 (d, <sup>3</sup>J<sub>H-H</sub> = 9.16 Hz, 4H), 3.10 (s, 12H). Because of the low solubility of **15**, a satisfactory <sup>13</sup>C NMR spectrum could not be obtained. HRMS (ESI/[M + H]<sup>+</sup>): calcd for C<sub>24</sub>H<sub>21</sub>Br<sub>2</sub>N<sub>4</sub>O<sub>2</sub> 555.0031, found 555.0026.

**Synthesis of 2,6-Dipyridin-4-yl-4,8-dibromobenzo[1,2-*d*;4,5-*d'*]bisoxazole (16).** In a 100 mL round-bottom flask equipped with a Friedrich condenser, compound **10** (2.45 g, 8.22 mmol) and isonicotinic acid (**13**, 3.07 g, 24.65 mmol) were mixed with polyphosphoric acid (20.0 g). The mixture was heated to 170 °C and stirred at that temperature for 25 h. After cooling, the suspension was neutralized with cold aqueous 1 M NaOH solution and filtered. The dark solid was washed with H<sub>2</sub>O, EtOH, and then Et<sub>2</sub>O. After air-drying, the solid was dissolved in 200 mL of a CH<sub>2</sub>Cl<sub>2</sub>/MeOH mixture (9:1) and then passed through a short silica gel column. Product was eluted using a CH<sub>2</sub>Cl<sub>2</sub>/MeOH/Et<sub>3</sub>N mixture (18:2:1). Solvent was removed in vacuo to give 2.09 g (54%, 4.42 mmol) of **16** (mp >350 °C, with decomposition). **16**. IR (neat): 1608 (w), 1576 (m), 1548 (m), 1490 (w), 1414 (s), 1357 (w), 1322 (m), 1279 (w), 1230 (s), 1060 (s), 990 (m), 971 (w), 920 (w), 876 (m), 830 (s), 740 (w),

723 (w), 697 (s), 687 (s)  $\text{cm}^{-1}$ .  $^1\text{H}$  NMR (THF- $d_8$ , 500 MHz):  $\delta$  8.86 (d,  $^3J_{\text{H-H}} = 5.73$  Hz, 4H), 8.18 (d,  $^3J_{\text{H-H}} = 5.73$  Hz, 4H).  $^{13}\text{C}$  NMR (THF- $d_8$ , 125 MHz):  $\delta$  163.9, 152.2, 148.6, 141.3, 134.0, 121.9, 93.6. HRMS (ESI/[M + H] $^+$ ): calcd for  $\text{C}_{18}\text{H}_9\text{Br}_2\text{N}_4\text{O}_2$  470.9092, found 470.9087.

**Synthesis of Cruciform 1.** Phenylacetylene (17, 391 mg, 3.83 mmol) was added to a thick-walled microwave pressure vial that contained a mixture of compound 14 (300 mg, 0.638 mmol),  $\text{PdCl}_2(\text{PPh}_3)_2$  (90 mg, 0.13 mmol), CuI (24 mg, 0.13 mmol),  $\text{NEt}_3$  (5 mL), and MeCN (5 mL). The vial was sealed and exposed to microwave irradiation for 3 h at 100 °C. After cooling, solvents were removed under reduced pressure, and the crude solid was purified by column chromatography, eluting first with pure  $\text{CH}_2\text{Cl}_2$  and then successively with  $\text{CH}_2\text{Cl}_2/\text{MeOH}$  mixtures in 97:3, 19:1, and 9:1 ratios. The solvent was removed under reduced pressure to give 270 mg (83%, 0.53 mmol) of 1 (mp 305 °C, with decomposition). 1. UV-vis ( $\text{CH}_2\text{Cl}_2$ ):  $\lambda_{\max}$  (log  $\epsilon$ ) = 304 (6.62), 367 (6.90) nm. IR (neat): 3067 (w,  $\tilde{\nu}_{\text{C-H}}$ ), 2221 (w,  $\tilde{\nu}_{\text{C=C}}$ ), 1609 (w), 1562 (m,  $\tilde{\nu}_{\text{O-C=N}}$ ), 1488 (m), 1451 (m), 1383 (w), 1340 (m), 1278 (m), 1079 (w), 1062 (m), 1027 (m), 977 (m), 918 (m), 777 (m), 755 (m), 723 (m), 697 (s), 687 (s)  $\text{cm}^{-1}$ .  $^1\text{H}$  NMR ( $\text{CDCl}_3$ , 500 MHz):  $\delta$  8.42 (m, 4H), 7.80 (m, 4H), 7.58 (m, 6H), 7.46 (m, 6H).  $^{13}\text{C}$  NMR ( $\text{CDCl}_3$ , 125 MHz):  $\delta$  164.8, 149.0, 141.1, 132.4, 132.3, 129.4, 129.2, 128.7, 128.4, 126.8, 123.0, 100.5, 98.9, 80.0. LRMS (ESI/[M + H] $^+$ ): calcd for  $\text{C}_{36}\text{H}_{21}\text{N}_2\text{O}_2$  513.15, found 513.33. HRMS: calcd for  $\text{C}_{36}\text{H}_{20}\text{N}_2\text{O}_2$  513.1603, found 513.1601. Anal. Calcd. for  $\text{C}_{36}\text{H}_{20}\text{N}_2\text{O}_2$ : C, 84.36; H, 3.93; N, 5.47. Found: C, 84.01; H, 3.52; N, 5.39.

**Synthesis of Cruciform 2.** In a nitrogen-flushed round-bottom flask, anhydrous  $\text{K}_2\text{CO}_3$  (1.06 g, 7.66 mmol) was added to a solution of 2-(4-(*N,N*-dimethylamino)phenyl)trimethylsilyl ethyne<sup>37</sup> (832 mg, 3.83 mmol) in a mixture of MeOH (5 mL) and THF (5 mL). After stirring for 30 min, the reaction mixture was filtered through Celite. The solvent was removed under reduced pressure to yield crude 4-ethynyl-*N,N*-dimethylaniline (18), which was used without purification in the next step. To minimize manipulations of this compound, we assumed a 95% yield for this reaction.

The entire amount of 18 (prepared as above-described) was added to a thick-walled microwave pressure vial that contained a mixture of compound 14 (300 mg, 0.638 mmol),  $\text{PdCl}_2(\text{PPh}_3)_2$  (90 mg, 0.13 mmol), CuI (24 mg, 0.13 mmol),  $\text{NEt}_3$  (5 mL), and MeCN (5 mL). The vial was sealed and exposed to microwave irradiation for 3 h at 100 °C. After cooling, solvents were removed under reduced pressure, and the crude solid was purified by column chromatography, eluting first with pure  $\text{CH}_2\text{Cl}_2$ , and then successively with  $\text{CH}_2\text{Cl}_2/\text{MeOH}$  mixtures in 97:3, 19:1, and 9:1 ratios. The solvent was removed under reduced pressure to give 338 mg (88%, 0.56 mmol) of pure 2 (mp >350 °C, with decomposition). 2. UV-vis ( $\text{CH}_2\text{Cl}_2$ ):  $\lambda_{\max}$  (log  $\epsilon$ ) = 279 (6.51), 317 (6.66), 342 (6.69), 356 (6.70), 374 (6.71), 443 (6.67) nm. IR (neat): 2890 (w,  $\tilde{\nu}_{\text{C-H}}$ ), 2853 (w,  $\tilde{\nu}_{\text{C-H}}$ ), 2801 (w,  $\tilde{\nu}_{\text{C-H}}$ ), 2211 (w,  $\tilde{\nu}_{\text{C=C}}$ ), 1606 (s), 1563 (m,  $\tilde{\nu}_{\text{O-C=N}}$ ), 1543 (m), 1512 (m), 1489 (m), 1452 (m), 1366 (m), 1353 (m), 1341 (m), 1315 (w), 1280 (m), 1227 (m), 1184 (s), 1169 (m), 1028 (m), 976 (m), 946 (m), 917 (m), 813 (s), 779 (m), 722 (m), 698 (s), 686 (s)  $\text{cm}^{-1}$ .  $^1\text{H}$  NMR ( $\text{CDCl}_3$ , 500 MHz):  $\delta$  8.42 (m, 4H), 7.67 (d,  $^3J_{\text{H-H}} = 9.16$  Hz, 4H), 7.56 (m, 6H), 6.74 (d,  $^3J_{\text{H-H}} = 9.16$  Hz, 4H), 3.06 (s, 12H).  $^{13}\text{C}$  NMR ( $\text{CDCl}_3$ , 125 MHz):  $\delta$  164.4, 150.8, 148.8, 141.5, 133.6, 132.0, 129.0, 128.3, 127.0, 111.9, 109.7, 102.9, 102.3, 78.5, 40.4. LRMS (ESI/[M + H] $^+$ ): calcd for  $\text{C}_{40}\text{H}_{31}\text{N}_4\text{O}_2$  599.24, found 599.33. HRMS: calcd for  $\text{C}_{40}\text{H}_{31}\text{N}_4\text{O}_2$  599.2447, found 599.2440. Anal. Calcd. for  $\text{C}_{40}\text{H}_{30}\text{N}_4\text{O}_2$ : C, 80.25; H, 5.05; N, 9.36. Found: C, 79.13; H, 4.52; N, 9.10. Despite three separate attempts, satisfactory elemental analysis for C and H could not be obtained.

**Synthesis of Cruciform 3.** In a nitrogen-flushed round-bottom flask, anhydrous  $\text{K}_2\text{CO}_3$  (1.06 g, 7.66 mmol) was added to a solution of 2-(4-(pyridinyl))trimethylsilyl ethyne<sup>38</sup> (671 mg, 3.83 mmol) in a mixture of MeOH (5 mL) and THF (5 mL). After being stirred for 30 min, the reaction mixture was filtered through Celite. The solvent was removed under reduced pressure to yield crude 4-ethynylpyridine (19), which was used without purification in the next step. To minimize manipulations of this somewhat sensitive compound, we assumed a 95% yield for this reaction.

The entire amount of 19 (prepared as above-described) was added to a thick-walled microwave pressure vial that contained a mixture of compound 14 (300 mg, 0.638 mmol),  $\text{PdCl}_2(\text{PPh}_3)_2$  (90 mg, 0.13 mmol), CuI (24 mg, 0.13 mmol),  $\text{NEt}_3$  (5 mL), and MeCN (5 mL). The vial was sealed and exposed to microwave irradiation for 3 h at 90 °C. After cooling, solvents were removed under reduced pressure, and the crude solid was purified by column chromatography, eluting first with pure  $\text{CH}_2\text{Cl}_2$ , and then successively with  $\text{CH}_2\text{Cl}_2/\text{MeOH}$  mixtures in 97:3, 19:1, and 9:1 ratios. The solvent was removed under reduced pressure to give 202 mg (62%, 0.39 mmol) of 3 (mp >350 °C, with decomposition). 3. UV-vis ( $\text{CH}_2\text{Cl}_2$ ):  $\lambda_{\max}$  (log  $\epsilon$ ) = 302 (6.52), 315 (6.52), 368 (6.76) nm. IR (neat): 2927 (w,  $\tilde{\nu}_{\text{C-H}}$ ), 2854 (w,  $\tilde{\nu}_{\text{C-H}}$ ), 2220 (w,  $\tilde{\nu}_{\text{C=C}}$ ), 1606 (s), 1591 (s), 1561 (m,  $\tilde{\nu}_{\text{O-C=N}}$ ), 1538 (w), 1486 (m), 1451 (m), 1407 (m), 1340 (m), 1280 (m), 1224 (m), 1210 (m), 1177 (w), 1160 (w), 1079 (m), 1064 (m), 1028 (m), 999 (w), 982 (m), 918 (m), 821 (s), 795 (m), 780 (m), 724 (m), 700 (s), 688 (s), 627 (m)  $\text{cm}^{-1}$ .  $^1\text{H}$  NMR ( $\text{CDCl}_3$ , 400 MHz):  $\delta$  8.72 (d,  $^3J_{\text{H-H}} = 4.12$  Hz, 4H), 8.38 (m, 4H), 7.63 (d,  $^3J_{\text{H-H}} = 5.95$  Hz, 4H), 7.58 (m, 6H).  $^{13}\text{C}$  NMR ( $\text{CDCl}_3$ , 100 MHz):  $\delta$  165.2, 150.1, 149.0, 141.4, 132.6, 130.9, 129.2, 128.4, 126.4, 126.1, 98.4, 97.5, 84.0. LRMS (ESI/[M + H] $^+$ ): calcd for  $\text{C}_{34}\text{H}_{19}\text{N}_4\text{O}_2$  515.14, found 515.2. HRMS: calcd for  $\text{C}_{34}\text{H}_{19}\text{N}_4\text{O}_2$  515.1508, found 515.1500. Anal. Calcd. for  $\text{C}_{34}\text{H}_{18}\text{N}_4\text{O}_2 \cdot ^1/4\text{CH}_2\text{Cl}_2$ : C, 76.78; H, 3.48; N, 10.46. Found: C, 77.19; H, 3.67; N, 10.46.

**Synthesis of Cruciform 4.** Phenylacetylene (17, 33 mg, 3.24 mmol) was added to a thick-walled microwave pressure vial that contained a mixture of compound 15 (300 mg, 0.54 mmol),  $\text{PdCl}_2(\text{PPh}_3)_2$  (76 mg, 0.11 mmol), CuI (21 mg, 0.11 mmol),  $\text{NEt}_3$  (5 mL), and MeCN (5 mL). The vial was sealed and exposed to microwave irradiation for 3 h at 100 °C. After cooling, solvents were removed under reduced pressure, and the crude solid was purified by column chromatography, eluting first with pure  $\text{CH}_2\text{Cl}_2$ , and then successively with  $\text{CH}_2\text{Cl}_2/\text{MeOH}$  mixtures in 97:3, 19:1, and 9:1 ratios. The solvent was removed under reduced pressure to give 232 mg (72%, 0.39 mmol) of cruciform 4 (mp >350 °C, with decomposition). 4. UV-vis ( $\text{CH}_2\text{Cl}_2$ ):  $\lambda_{\max}$  (log  $\epsilon$ ) = 335 (6.62), 378 (6.53), 437 (6.67) nm. IR (neat): 2904 (w,  $\tilde{\nu}_{\text{C-H}}$ ), 2220 (w,  $\tilde{\nu}_{\text{C=C}}$ ), 1607 (s), 1585 (m), 1509 (s), 1487 (w), 1444 (m), 1436 (m), 1368 (m), 1355 (m), 1337 (m), 1281 (w), 1185 (s), 1065 (m), 976 (m), 944 (w), 910 (m), 815 (m), 762 (m), 741 (m), 691 (m)  $\text{cm}^{-1}$ .  $^1\text{H}$  NMR ( $\text{CDCl}_3$ , 400 MHz):  $\delta$  8.25 (d,  $^3J_{\text{H-H}} = 9.16$  Hz, 4H), 7.79 (m, 4H), 7.43 (m, 6H), 6.79 (d,  $^3J_{\text{H-H}} = 9.16$  Hz, 4H), 3.10 (s, 12H).  $^{13}\text{C}$  NMR ( $\text{CDCl}_3$ , 100 MHz):  $\delta$  165.6, 152.7, 148.8, 140.8, 132.4, 129.8, 129.0, 128.6, 123.4, 113.9, 111.7, 99.5, 97.3, 80.7, 40.4. LRMS (ESI/[M + H] $^+$ ): calcd for  $\text{C}_{40}\text{H}_{31}\text{N}_4\text{O}_2$  599.24, found 599.33. HRMS: calcd for  $\text{C}_{40}\text{H}_{31}\text{N}_4\text{O}_2$  599.2447, found 599.2444. Anal. Calcd. for  $\text{C}_{40}\text{H}_{30}\text{N}_4\text{O}_2 \cdot ^1/3\text{CH}_2\text{Cl}_2$ : C, 77.26; H, 4.93; N, 8.94. Found: C, 77.67; H, 4.62; N, 8.78. Despite repeated attempts, satisfactory elemental analysis for C could not be obtained.

**Synthesis of Cruciform 5.** Compound 18 (261 mg, 1.80 mmol) was added to a thick-walled pressure vessel that contained a mixture of compound 15 (100 mg, 0.18 mmol),  $\text{PdCl}_2(\text{PPh}_3)_2$  (25 mg, 0.036 mmol), CuI (7 mg, 0.036 mmol), i-Pr<sub>2</sub>NH (2 mL), and MeCN (2 mL). The vessel was sealed, and the mixture was heated for 7 days at 120 °C. After cooling, solvents were removed under reduced pressure, and the crude solid was purified by column chromatography, eluting first with pure  $\text{CH}_2\text{Cl}_2$  and then successively with  $\text{CH}_2\text{Cl}_2/\text{MeOH}$  mixtures in 97:3, 19:1, and 9:1 ratios. The solvent was removed under reduced pressure to give 51 mg (41%, 0.074 mmol) of cruciform 5 (mp >350 °C, with decomposition). 5. UV-vis ( $\text{CH}_2\text{Cl}_2$ ):  $\lambda_{\max}$  (log  $\epsilon$ ) = 310 (6.76), 334 (6.67), 421 (7.08) nm. IR (neat): 2910 (w,  $\tilde{\nu}_{\text{C-H}}$ ), 2212 (w,  $\tilde{\nu}_{\text{C=C}}$ ), 1607 (s), 1586 (w), 1540 (w), 1509 (s), 1445 (w), 1364 (m), 1339 (m), 1284 (w), 1230 (w), 1184 (m), 1066 (w), 975 (w), 945 (w), 911 (w), 814 (m), 741 (w), 695 (w)  $\text{cm}^{-1}$ .  $^1\text{H}$  NMR ( $\text{CDCl}_3$ , 500 MHz):  $\delta$  8.25 (d,  $^3J_{\text{H-H}} = 9.16$  Hz, 4H), 7.66 (d,  $^3J_{\text{H-H}} = 8.59$  Hz, 4H), 6.79 (d,  $^3J_{\text{H-H}} = 8.59$  Hz, 4H), 6.73 (d,  $^3J_{\text{H-H}} = 9.16$  Hz, 4H), 3.09 (s, 12H), 3.04 (s, 12H). Because of the low solubility of cruciform 5, a satisfactory  $^{13}\text{C}$  NMR spectrum could not be obtained. LRMS (ESI/[M + H] $^+$ ): calcd for  $\text{C}_{44}\text{H}_{41}\text{N}_6\text{O}_2$  685.32, found 685.50. HRMS: calcd for  $\text{C}_{44}\text{H}_{41}\text{N}_6\text{O}_2$  685.3291, found 685.3289. Anal. Calcd for

$C_{44}H_{40}N_6O_2 \cdot 2CH_2Cl_2$ : C, 64.64; H, 5.19; N, 9.83. Found: C, 64.62; H, 5.41; N, 9.74.

**Synthesis of Cruciform 6.** Compound **19** (56 mg, 0.54 mmol) was added to a thick-walled microwave pressure vial that contained a mixture of compound **15** (100 mg, 0.18 mmol),  $PdCl_2(PPh_3)_2$  (25 mg, 0.036 mmol),  $CuI$  (7 mg, 0.036 mmol),  $NEt_3$  (2 mL), and MeCN (2 mL). The vial was sealed and exposed to microwave irradiation for 3 h at 120 °C. After cooling, solvents were removed under reduced pressure, and the crude solid was purified by column chromatography, eluting first with pure  $CH_2Cl_2$ , and then successively with  $CH_2Cl_2/MeOH$  mixtures in 97:3, 19:1, and 9:1 ratios. The solvents were removed under reduced pressure to give 32 mg (30%, 0.053 mmol) of compound **6** (mp >350 °C, with decomposition). **6**: UV-vis ( $CH_2Cl_2$ ):  $\lambda_{max}$  (log  $\epsilon$ ) = 347 (6.92), 458 (6.81) nm. IR (neat): 2907 (w,  $\tilde{\nu}_{C-H}$ ), 2224 (w,  $\tilde{\nu}_{C\equiv C}$ ), 1608 (s), 1593 (m), 1508 (s), 1488 (w), 1448 (w), 1434 (w), 1408 (w), 1365 (m), 1337 (m), 1282 (w), 1224 (w), 1192 (m), 1170 (w), 1074 (m), 980 (m), 944 (w), 913 (m), 820 (s), 743 (m), 698 (w) cm<sup>-1</sup>. <sup>1</sup>H NMR ( $CDCl_3$ , 500 MHz):  $\delta$  8.71 (d, <sup>3</sup> $J_{H-H}$  = 5.73 Hz, 4H), 8.23 (d, <sup>3</sup> $J_{H-H}$  = 9.16 Hz, 4H), 7.64 (d, <sup>3</sup> $J_{H-H}$  = 5.73 Hz, 4H), 6.80 (d, <sup>3</sup> $J_{H-H}$  = 9.16 Hz, 4H), 3.11 (s, 12H). <sup>13</sup>C NMR ( $CDCl_3$ , 125 MHz):  $\delta$  166.0, 153.0, 150.1, 147.6, 141.1, 137.6, 129.9, 126.1, 113.4, 111.7, 85.0, 40.3 (one peak is missing; poor solubility of this compound precluded the collection of a better <sup>13</sup>C NMR spectrum). LRMS (ESI/[M + H]<sup>+</sup>): calcd for  $C_{38}H_{29}N_6O_2$  601.23, found 601.30. HRMS: calcd for  $C_{38}H_{29}N_6O_2$  601.2352, found 601.2343. Anal. Calcd. for  $C_{38}H_{28}N_6O_2 \cdot 1/3CH_2Cl_2$ : C, 73.20; H, 4.59; N, 13.36. Found: C, 73.02; H, 4.17; N, 13.26.

**Synthesis of Cruciform 7.** Phenylacetylene (**17**, 95  $\mu$ L, 0.85 mmol) was added to a thick-walled microwave pressure vial that contained a mixture of compound **16** (100 mg, 0.21 mmol),  $PdCl_2(PPh_3)_2$  (30 mg, 0.042 mmol),  $CuI$  (8 mg, 0.042 mmol),  $NEt_3$  (2 mL), and MeCN (2 mL). The vial was sealed and exposed to microwave irradiation for 3 h at 100 °C. After cooling, solvents were removed under reduced pressure, and the crude solid was purified by column chromatography, eluting first with pure  $CH_2Cl_2$  and then successively with  $CH_2Cl_2/MeOH$  mixtures in 97:3, 19:1, and 9:1 ratios. The solvent was removed under reduced pressure to give 28 mg (26%, 0.054 mmol) of pure **7** (mp >350 °C, with decomposition). **7**: UV-vis ( $CH_2Cl_2$ ):  $\lambda_{max}$  (log  $\epsilon$ ) = 311 (6.40), 367 (6.51) nm. IR (neat): 3061 (w,  $\tilde{\nu}_{C-H}$ ), 2214 (w,  $\tilde{\nu}_{C\equiv C}$ ), 1597 (m), 1576 (m), 1546 (m), 1489 (m), 1442 (m), 1414 (m), 1394 (w), 1339 (m), 1283 (m), 1216 (w), 1064 (m), 1028 (w), 991 (m), 981 (m), 924 (m), 831 (m), 755 (s), 691 (s) cm<sup>-1</sup>. <sup>1</sup>H NMR ( $CDCl_3$ , 500 MHz):  $\delta$  8.89 (br s, 4H), 8.25 (br d, <sup>3</sup> $J_{H-H}$  = 4.01 Hz, 4H), 7.80 (m, 4H), 7.47 (m, 4H). Because of the poor solubility of **7**, a satisfactory <sup>13</sup>C NMR spectrum could not be obtained. HRMS (ESI/[M + H]<sup>+</sup>): calcd for  $C_{34}H_{19}N_4O_2$  515.1508, found 515.1502. Anal. Calcd for  $C_{34}H_{18}N_4O_2 \cdot CH_2Cl_2$ : C, 70.12; H, 3.36; N, 9.35. Found: C, 70.17; H, 2.96; N, 7.80. Despite three separate attempts, satisfactory elemental analysis for N could not be obtained.

**Synthesis of Cruciform 8.** Compound **18** (157 mg, 1.06 mmol) was added to a thick-walled microwave pressure vial that contained a mixture of compound **16** (100 mg, 0.21 mmol),  $PdCl_2(PPh_3)_2$  (30 mg, 0.042 mmol),  $CuI$  (8 mg, 0.042 mmol),  $NEt_3$  (2 mL), and MeCN (2 mL). The vial was sealed and exposed to microwave irradiation for 3 h at 110 °C. After cooling, solvents were removed under reduced pressure, and the crude solid was purified by column chromatography, eluting first with pure  $CH_2Cl_2$ , and then successively with  $CH_2Cl_2/MeOH$  mixtures in 97:3, 19:1, and 9:1 ratios. The solvent was removed under reduced pressure to give 27 mg (21%, 0.045 mmol) of compound **8** (mp >350 °C, with decomposition). **8**: UV-vis ( $CH_2Cl_2$ ):  $\lambda_{max}$  (log  $\epsilon$ ) = 277 (6.28), 332 (6.52), 350 (6.60), 368 (6.57), 468 (6.36) nm. IR (neat): 2891 (w,  $\tilde{\nu}_{C-H}$ ), 2120 (w,  $\tilde{\nu}_{C\equiv C}$ ), 1606 (s), 1578 (w), 1544 (m), 1518 (m), 1486 (w), 1445 (w), 1415 (w), 1356 (m), 1287 (w), 1229 (w), 1186 (m), 1168 (m), 1130 (w), 1063 (w), 991 (w), 980 (w), 946 (w), 927 (w), 817 (m), 740 (w), 725 (w), 699 (w), 690 (w) cm<sup>-1</sup>. <sup>1</sup>H NMR ( $CDCl_3$ , 500 MHz):  $\delta$  8.87 (d, <sup>3</sup> $J_{H-H}$  = 6.30 Hz, 4H), 8.25 (d, <sup>3</sup> $J_{H-H}$  = 6.30 Hz, 4H), 7.66 (d, <sup>3</sup> $J_{H-H}$  = 9.16 Hz, 4H), 6.75 (d, <sup>3</sup> $J_{H-H}$  = 9.16 Hz, 4H), 3.07 (s, 12H). Because of the poor solubility of **8**, a satisfactory <sup>13</sup>C NMR spectrum could not be

obtained. LRMS (ESI/[M + H]<sup>+</sup>): calcd for  $C_{38}H_{28}N_6O_2$  601.23, found 601.30. HRMS: calcd for  $C_{38}H_{29}N_6O_2$  601.2352, found 601.2350. Anal. Calcd for  $C_{38}H_{28}N_6O_2 \cdot CH_2Cl_2$ : C, 68.32; H, 4.41; N, 12.26. Found: C, 69.67; H, 4.04; N, 12.46. Inclusion of dichloromethane was confirmed by an X-ray crystal structure. Despite repeated attempts, satisfactory elemental analysis for C could not be obtained.

**Synthesis of Cruciform 9.** Compound **19** (262 mg, 2.54 mmol) was added to a thick-walled microwave pressure vial that contained a mixture of compound **16** (300 mg, 0.64 mmol),  $PdCl_2(PPh_3)_2$  (89 mg, 0.13 mmol),  $CuI$  (24 mg, 0.13 mmol), *i*-Pr<sub>2</sub>NH (4 mL), and MeCN (4 mL). The vial was sealed and exposed to microwave irradiation for 4 h at 115 °C. After cooling, solvents were removed under reduced pressure, and the crude solid was purified by column chromatography, eluting first with pure  $CH_2Cl_2$ , and then successively with  $CH_2Cl_2/MeOH$  mixtures in 97:3, 19:1, and 9:1 ratios. The solvent was removed under reduced pressure to give 28 mg (8.5%, 0.054 mmol) of pure **9** (mp >350 °C, with decomposition). **9**: UV-vis ( $CH_2Cl_2$ ):  $\lambda_{max}$  (log  $\epsilon$ ) = 304 (6.18), 315 (6.18), 367 (6.34) nm. IR (neat): 3040 (w,  $\tilde{\nu}_{C-H}$ ), 2221 (w,  $\tilde{\nu}_{C\equiv C}$ ), 1591 (s), 1575 (m), 1545 (m), 1486 (w), 1409 (m), 1384 (w), 1339 (m), 1318 (w), 1283 (w), 1228 (w), 1207 (w), 1061 (m), 992 (m), 984 (m), 922 (m), 829 (s), 817 (s), 740 (m), 726 (m), 699 (m), 689 (m) cm<sup>-1</sup>. <sup>1</sup>H NMR ( $CDCl_3$ , 400 MHz):  $\delta$  8.91 (d, <sup>3</sup> $J_{H-H}$  = 5.95 Hz, 4H), 8.76 (d, <sup>3</sup> $J_{H-H}$  = 5.95 Hz, 4H), 8.25 (d, <sup>3</sup> $J_{H-H}$  = 5.95 Hz, 4H), 7.65 (d, <sup>3</sup> $J_{H-H}$  = 5.95 Hz, 4H). <sup>13</sup>C NMR ( $CDCl_3$ , 100 MHz):  $\delta$  163.2, 151.2, 150.3, 149.3, 141.8, 133.4, 130.4, 126.0, 121.6, 99.6, 98.5, 83.1. LRMS (ESI/[M + H]<sup>+</sup>): calcd for  $C_{32}H_{17}N_6O_2$  517.13, found 517.20.

## ASSOCIATED CONTENT

### S Supporting Information

Additional experimental and computational details, copies of NMR spectra for all new compounds, and crystallographic information files (CIFs) for **1**, **2**, and **8**. This material is available free of charge via the Internet at <http://pubs.acs.org>.

## AUTHOR INFORMATION

### Corresponding Author

\*E-mail: miljanic@uh.edu

## ACKNOWLEDGMENTS

This research was financially supported by the grants made to O.Š.M. by the Welch Foundation (Grant No. E-1768), the donors of the American Chemical Society Petroleum Research Fund (ACS-PRF), the University of Houston (UH), and its grant to Advance and Enhance Research, and the Texas Center for Superconductivity at UH. Ms. Thao Shirley Nguyen and Dr. Karolina Osowska (UH) are acknowledged for assistance with synthesis of **1**. We thank Prof. Rigoberto Advincula (UH) for access to his fluorimetry equipment, and Jacob Armitage (Texas State University) for his help with X-ray data collection. Crystallographic equipment at Texas State University was acquired through support from the National Science Foundation (CHE-0821254).

## REFERENCES

- (a) *Functional Organic Materials: Syntheses, Strategies and Applications*; Müller, T. J., Bunz, U. H. F., Eds.; Wiley-VCH: Weinheim, 2007. (b) *Electronic Materials, the Oligomer Approach*; Müllen, K., Wegner, G., Eds.; Wiley-VCH: Weinheim, 1998. (c) Fukui, K. *Science* **1982**, 218, 747–754.
- For examples of noncruciform structures with spatially separated FMOs, see: (a) Fahrni, C. J.; Yang, L.; VanDerveer, D. G. *J. Am. Chem. Soc.* **2003**, 125, 3799–3812. (b) Huang, H.-H.; Prabhakar, Ch.; Tang, K.-C.; Chou, P.-T.; Huang, G.-J.; Yang, J.-S. *J. Am. Chem. Soc.* **2011**, 133, 8028–8039.

- (3) (a) Ohta, K.; Yamada, S.; Kamada, K.; Slepkov, A. D.; Hegmann, F. A.; Tykwinski, R. R.; Shirtcliff, L. D.; Haley, M. M.; Salek, P.; Gel'mukhanov, F.; Ågren, H. *J. Phys. Chem. A* **2011**, *115*, 105–117. (b) Carroll, C. N.; Naleway, J. J.; Haley, M. M.; Johnson, D. W. *Chem. Soc. Rev.* **2010**, *39*, 3875–3888. (c) Spitler, E. L.; Haley, M. M. *Tetrahedron* **2008**, *64*, 11469–11474. (d) Spitler, E. L.; Monson, J. M.; Haley, M. M. *J. Org. Chem.* **2008**, *73*, 2211–2223. (e) Spitler, E. L.; Shirtcliff, L. D.; Haley, M. M. *J. Org. Chem.* **2007**, *72*, 86–96. (f) Bhaskar, A.; Guda, R.; Haley, M. M.; Goodson, T. III. *J. Am. Chem. Soc.* **2006**, *128*, 13972–13973. (g) Marsden, J. A.; Miller, J. J.; Shirtcliff, L. D.; Haley, M. M. *J. Am. Chem. Soc.* **2005**, *127*, 2464–2476. (h) Miller, J. J.; Marsden, J. A.; Haley, M. M. *Synlett* **2004**, 165–168.
- (4) (a) Davey, E. A.; Zuccherio, A. J.; Trapp, O.; Bunz, U. H. F. *J. Am. Chem. Soc.* **2011**, *133*, 7716–7718. (b) McGrier, P. L.; Solntsev, K. M.; Zuccherio, A. J.; Miranda, O. R.; Rotello, V. M.; Tolbert, L. M.; Bunz, U. H. F. *Chem.—Eur. J.* **2011**, *17*, 3112–3119. (c) Zuccherio, A. J.; McGrier, P. L.; Bunz, U. H. F. *Acc. Chem. Res.* **2010**, *43*, 397–408. (d) Tolosa, J.; Solntsev, K. M.; Tolbert, L. M.; Bunz, U. H. F. *J. Org. Chem.* **2010**, *75*, 523–534. (e) Zuccherio, A. J.; Shiels, R. A.; McGrier, P. L.; To, M. A.; Jones, C. W.; Bunz, U. H. F. *Chem.—Asian J.* **2009**, *4*, 262–269. (f) Tolosa, J.; Bunz, U. H. F. *Chem.—Asian J.* **2009**, *4*, 270–276. (g) McGrier, P. L.; Solntsev, K. M.; Miao, S.; Tolbert, L. M.; Miranda, O. R.; Rotello, V. M.; Bunz, U. H. F. *Chem.—Eur. J.* **2008**, *14*, 4503–4510. (h) Tolosa, J.; Zuccherio, A. J.; Bunz, U. H. F. *J. Am. Chem. Soc.* **2008**, *130*, 6498–6506. (i) Brumbosz, S. M.; Zuccherio, A. J.; Phillips, R. L.; Vasquez, D.; Wilson, A.; Bunz, U. H. F. *Org. Lett.* **2007**, *9*, 4519–4522. (j) Hauck, M.; Schönhaber, J.; Zuccherio, A. J.; Hardcastle, K. I.; Müller, T. J. J.; Bunz, U. H. F. *J. Org. Chem.* **2007**, *72*, 6714–6725. (k) McGrier, P. L.; Solntsev, K. M.; Schönhaber, J.; Brumbosz, S. M.; Tolbert, L. M.; Bunz, U. H. F. *Chem. Commun.* **2007**, 2127–2129. (l) Zuccherio, A. J.; Wilson, J. N.; Bunz, U. H. F. *J. Am. Chem. Soc.* **2006**, *128*, 11872–11881. (m) Gerhardt, W. W.; Zuccherio, A. J.; Wilson, J. N.; South, C. R.; Bunz, U. H. F.; Weck, M. *Chem. Commun.* **2006**, 2141–2143. (n) Wilson, J. N.; Bunz, U. H. F. *J. Am. Chem. Soc.* **2005**, *127*, 4124–4125. (o) Wilson, J. N.; Smith, M. D.; Enkelmann, V.; Bunz, U. H. F. *Chem. Commun.* **2004**, 1700–1701. (p) Wilson, J. N.; Hardcastle, K. I.; Josowicz, M.; Bunz, U. H. F. *Tetrahedron* **2004**, *60*, 7157–7167. (q) Wilson, J. N.; Josowicz, M.; Wang, Y.; Bunz, U. H. F. *Chem. Commun.* **2003**, 2962–2963.
- (5) Kang, H.; Evmenenko, G.; Dutta, P.; Clays, K.; Song, K.; Marks, T. J. *J. Am. Chem. Soc.* **2006**, *128*, 6194–6205. (b) Kang, H.; Zhu, P.; Yang, Y.; Facchetti, A.; Marks, T. J. *J. Am. Chem. Soc.* **2004**, *126*, 15974–15975.
- (6) (a) Gisselbrecht, J. P.; Moonen, N. N. P.; Boudon, C.; Nielsen, M. B.; Diederich, F.; Gross, M. *Eur. J. Org. Chem.* **2004**, 2959–2972. (b) Mitzel, F.; Boudon, C.; Gisselbrecht, J. P.; Seiler, P.; Gross, M.; Diederich, F. *Helv. Chim. Acta* **2004**, *87*, 1130–1157. (c) Diederich, F. *Chem. Commun.* **2001**, 219–227. (d) Gobbi, L.; Seiler, P.; Diederich, F. *Angew. Chem., Int. Ed.* **1999**, *38*, 674–678. (e) Hilger, A.; Gisselbrecht, J.-P.; Tykwinski, R. R.; Boudon, C.; Schreiber, M.; Martin, R. E.; Lüthi, H. P.; Gross, M.; Diederich, F. *J. Am. Chem. Soc.* **1997**, *119*, 2069–2078. (f) Bosshard, C.; Spreiter, R.; Günter, P.; Tykwinski, R. R.; Schreiber, M.; Diederich, F. *Adv. Mater.* **1996**, *8*, 231–234. (g) Tykwinski, R. R.; Schreiber, M.; Carlon, R. P.; Diederich, F.; Gramlich, V. *Helv. Chim. Acta* **1996**, *79*, 2249–2281. (h) Anthony, J.; Boldi, A. M.; Rubin, Y.; Hob, M.; Gramlich, V.; Knobler, C. B.; Seiler, P.; Diederich, F. *Helv. Chim. Acta* **1995**, *78*, 13–45. See also: (i) Zhao, Y. M.; Tykwinski, R. R. *J. Am. Chem. Soc.* **1999**, *121*, 458–459. (j) Eisler, S.; Tykwinski, R. R. *J. Am. Chem. Soc.* **2000**, *122*, 10736–10737. (k) Zhao, Y. M.; Ciulei, S. C.; Tykwinski, R. R. *Tetrahedron Lett.* **2001**, *42*, 7721–7723.
- (7) (a) Koenen, J.-M.; Bilge, A.; Allard, S.; Alle, R.; Meerholz, K.; Scherf, U. *Org. Lett.* **2009**, *11*, 2149–2152. (b) Pina, J.; Seixas de Melo, J.; Burrows, H. D.; Galbrecht, F.; Bilge, A.; Kudla, C. J.; Scherf, U. *J. Phys. Chem. B* **2008**, *112*, 1104–1111. (c) Zen, A.; Bilge, A.; Galbrecht, F.; Alle, R.; Meerholz, K.; Grenzer, J.; Neher, D.; Scherf, U.; Farrell, T. *J. Am. Chem. Soc.* **2006**, *128*, 3914–3915. (d) Bilge, A.; Zen, A.; Forster, M.; Li, H.; Galbrecht, F.; Nehls, B. S.; Farrell, T.; Neher, D.; Scherf, U. *J. Mater. Chem.* **2006**, *16*, 3177–3182.
- (8) Mangalam, A.; Gilliard, R. J. Jr.; Hanley, J. M.; Parke, A. M.; Smith, R. C. *Org. Biomol. Chem.* **2010**, *8*, 5620–5627.
- (9) Hu, J.-y.; Era, M.; Elsegood, M. R. J.; Yamato, T. *Eur. J. Org. Chem.* **2010**, 72–79.
- (10) Cho, M. J.; Park, S. S.; Yang, Y. S.; Kim, J. H.; Choi, D. H. *Synth. Met.* **2010**, *160*, 1754–1760.
- (11) (a) Grunder, S.; Huber, R.; Wu, S.; Schönenberger, C.; Calame, M.; Mayor, M. *Chimia* **2010**, *64*, 140–144. (b) Grunder, S.; Huber, R.; Wu, S.; Schönenberger, C.; Calame, M.; Mayor, M. *Eur. J. Org. Chem.* **2010**, 833–845. (c) Grunder, S.; Huber, R.; Horhoiu, V.; González, M. T.; Schönenberger, C.; Calame, M.; Mayor, M. *J. Org. Chem.* **2007**, *72*, 8337–8343. (d) Błaszczyk, A.; Fischer, M.; von Hänisch, C.; Mayor, M. *Eur. J. Org. Chem.* **2007**, 2630–2642.
- (12) (a) Jenum, K.; Vestergaard, M.; Pedersen, A. H.; Fock, J.; Jensen, J.; Santella, M.; Led, J. J.; Kilså, K.; Bjørnholm, T.; Nielsen, M. B. *Synthesis* **2011**, 539–548. (b) Vestergaard, M.; Jenum, K.; Sørensen, J. K.; Kilså, K.; Nielsen, M. B. *J. Org. Chem.* **2008**, *73*, 3175–3183. (c) Sørensen, J. K.; Vestergaard, M.; Kadziola, A.; Kilså, K.; Nielsen, M. B. *Org. Lett.* **2006**, *8*, 1173–1176.
- (13) In this paper, “benzobisoxazole” will be used in this to denote “benzo[1,2-d:4,5-d']bisoxazole”, the systematic name for the central heterocyclic core of the prepared cruciforms **1–9**, their precursors **14–16**, and compound **20**.
- (14) For structurally related fluorescent benzobisimidazoles (which are not cruciform-shaped), see: (a) Boydston, A. J.; Pecinovsky, C. S.; Chao, S. T.; Bielawski, C. W. *J. Am. Chem. Soc.* **2007**, *129*, 14550–14551. (b) Boydston, A. J.; Vu, P. D.; Dykno, O. L.; Chang, V.; Wyatt, A. R. II; Stockett, A. S.; Ritschdorff, E. T.; Shear, J. B.; Bielawski, C. W. *J. Am. Chem. Soc.* **2008**, *130*, 3143–3156. (c) Boydston, A. J.; Khramov, D. M.; Bielawski, C. W. *Tetrahedron Lett.* **2006**, *47*, 5123–5125. (d) Khramov, D. M.; Boydston, A. J.; Bielawski, C. W. *Org. Lett.* **2006**, *8*, 1831–1834.
- (15) (a) Klare, J. E.; Tulevski, G. S.; Nuckolls, C. *Langmuir* **2004**, *20*, 10068–10072. (b) Klare, J. E.; Tulevski, G. S.; Sugo, K.; de Picciotto, A.; White, K. A.; Nuckolls, C. *J. Am. Chem. Soc.* **2003**, *125*, 6030–6031. The latter reference also pioneered the use of the phrase “molecular cruciforms”. See also: (c) Tlach, B. C.; Tomlinson, A. L.; Bhuvalka, A.; Jeffries-EL, M. *J. Org. Chem.* **2011**, *76*, 8670–8681.
- (16) (a) Feldman, A. K.; Steigerwald, M. L.; Guo, X.; Nuckolls, C. *Acc. Chem. Res.* **2008**, *41*, 1731–1741. (b) Tang, J.; Wang, Y.; Klare, J. E.; Tulevski, G. S.; Wind, S. J.; Nuckolls, C. *Angew. Chem., Int. Ed.* **2007**, *46*, 3892–3895. (c) Florio, G. M.; Klare, J. E.; Pasamba, M. O.; Werblowsky, T. L.; Hyers, M.; Berne, B. J.; Hybertsen, M. S.; Nuckolls, C.; Flynn, G. W. *Langmuir* **2006**, *22*, 10003–10008. (d) Guo, X.; Small, J. P.; Klare, J. E.; Wang, Y.; Purewal, M. S.; Tam, I. W.; Hong, B. H.; Caldwell, R.; Huang, L.; O'Brien, S.; Yan, J.; Breslow, R.; Wind, S. J.; Hone, J.; Kim, P.; Nuckolls, C. *Science* **2006**, *311*, 356–359. (e) de Picciotto, A.; Klare, J. E.; Nuckolls, C.; Baldwin, K.; A Erbe, A.; Willett, R. *Nanotechnology* **2005**, *16*, 3110–3114.
- (17) Osowska, K.; Miljanic, O. Š. *Chem. Commun.* **2010**, *46*, 4276–4278.
- (18) (a) Hegedus, L. S.; Odle, R. R.; Winton, P. M.; Weider, P. R. *J. Org. Chem.* **1982**, *47*, 2607–2613. See also: (b) Weider, P. R.; Hegedus, L. S.; Asada, H.; D'Andrea, S. V. *J. Org. Chem.* **1985**, *50*, 4276–4281. (c) Osman, A.-M.; Bassiouni, I. *J. Org. Chem.* **1962**, *27*, 558–561.
- (19) (a) Wolfe, J. F.; Arnold, F. E. *Macromolecules* **1981**, *14*, 909–915. (b) Perry, R. J.; Wilson, B. D.; Miller, R. J. *J. Org. Chem.* **1992**, *57*, 2883–2887. (c) Seha, Z.; Weis, C. D. *Helv. Chim. Acta* **1980**, *63*, 413–419.
- (20) (a) Kappe, C. O. *Angew. Chem., Int. Ed.* **2004**, *43*, 6250–6284. (b) Lidström, P.; Tierney, J.; Wathey, B.; Westman, J. *Tetrahedron* **2001**, *57*, 9225–9283.
- (21) (a) Sonogashira, K. In *Handbook of Organopalladium Chemistry for Organic Synthesis*; Negishi, E.-i., Ed.; Wiley: New York, 2002; Vol. 1, p 493 and references cited therein. (b) Sonogashira, K.; Tohda, Y.; Hagihara, N. *Tetrahedron Lett.* **1975**, *16*, 4467–4470.
- (22) Gaussian 09, Revision B.01; Frisch, M. J.; Trucks, G. W.; Schlegel, H. B.; Scuseria, G. E.; Robb, M. A.; Cheeseman, J. R.; Scalmani, G.;

Barone, V.; Mennucci, B.; Petersson, G. A.; Nakatsuji, H.; Caricato, M.; Li, X.; Hratchian, H. P.; Izmaylov, A. F.; Bloino, J.; Zheng, G.; Sonnenberg, J. L.; Hada, M.; Ehara, M.; Toyota, K.; Fukuda, R.; Hasegawa, J.; Ishida, M.; Nakajima, T.; Honda, Y.; Kitao, O.; Nakai, H.; Vreven, T.; Montgomery, J. A., Jr.; Peralta, J. E.; Ogliaro, F.; Bearpark, M.; Heyd, J. J.; Brothers, E.; Kudin, K. N.; Staroverov, V. N.; Keith, T.; Kobayashi, R.; Normand, J.; Raghavachari, K.; Rendell, A.; Burant, J. C.; Iyengar, S. S.; Tomasi, J.; Cossi, M.; Rega, N.; Millam, J. M.; Klene, M.; Knox, J. E.; Cross, J. B.; Bakken, V.; Adamo, C.; Jaramillo, J.; Gomperts, R.; Stratmann, R. E.; Yazyev, O.; Austin, A. J.; Cammi, R.; Pomelli, C.; Ochterski, J. W.; Martin, R. L.; Morokuma, K.; Zakrzewski, V. G.; Voth, G. A.; Salvador, P.; Dannenberg, J. J.; Dapprich, S.; Daniels, A. D.; Farkas, O.; Foresman, J. B.; Ortiz, J. V.; Cioslowski, J.; Fox, D. J. Gaussian, Inc., Wallingford, CT, 2010.

(23) (a) Becke, A. D. *J. Chem. Phys.* **1993**, *98*, 5648–5652. (b) Lee, C.; Yang, W.; Parr, G. R. *Phys. Rev. B* **1988**, *37*, 785–789.

(24) This definition is analogous to the definition of, e.g., percent enantiomeric excess: Eliel, E. L.; Wilen, S. H.; Mander, L. N. *Stereochemistry of Organic Compounds*; Wiley: New York, 1994; p 214. We have also recalculated orbitals of **8** using a 6-311+G basis set. The densities of the HOMO and LUMO were compared to those computed at the 3-21G level. The standard deviation for the differences of the densities for these two basis sets was computed to be only 0.031 electrons with a variance of 0.001. Thus, the 3-21G values were used in this study.

(25) For a collection of  $pK_a$  values, see [www.zirchrom.com/organic.html](http://www.zirchrom.com/organic.html) and [www.scripps.edu/chem/baran/heterocycles/Essentials\\_1-2009.pdf](http://www.scripps.edu/chem/baran/heterocycles/Essentials_1-2009.pdf). Protonation of oxazole ( $pK_a = 0.8$ ) can be ignored, except in highly acidic solutions.

(26) Simple FMO arguments are very useful in predicting the optical response to protonation of pyridyl and 4-(dimethylamino) groups along cruciforms' "arms". However, these arguments are not easily applied to the protonation of the oxazole ring, as both HOMO and LUMO invariably have high orbital densities within that ring. At present, we have no explanation as to why this presumed protonation affects emission but not absorption.

(27) Tentatively,  $^1\text{H}$  NMR spectroscopy supports this assignment of protonation order, although solubility issues precluded us from following protonation-induced NMR changes over the range of  $-\log[\text{TFA}]$  values used in absorption and fluorescence studies.

(28) In the only other benzobisoxazole-related entry in the Cambridge Structural Database (CSD), only the unit cell and space group have been determined for 4,8-dichloro-2,6-diethylbenzo(1–2,4–5)bisoxazole. See: Roldan, L. G.; Litt, M. H. *Acta Crystallogr. Sect. B* **1968**, *B24*, 1394.

(29) Crystal structure data have been deposited with the Cambridge Crystallographic Data Centre under CCDC codes 828252 (1), 828253 (2), and 828254 (8). These data can be obtained free of charge from the Cambridge Crystallographic Data Centre via [www.ccdc.cam.ac.uk/data\\_request/cif](http://www.ccdc.cam.ac.uk/data_request/cif).

(30) Spek, A. L. *PLATON/SQUEEZE—A Multipurpose Crystallographic Tool*, Utrecht University, 2000.

(31) These angles were defined by (1) the atom of the  $\text{C}\equiv\text{C}$  bond directly attached to the phenyl ring of the benzobisoxazole, (2) the centroid of the central phenyl ring, and (3) the atom of the "horizontal" substituent directly attached to the oxazole ring of the benzobisoxazole core.

(32) Hunter, C. A.; Sanders, J. K. M. *J. Am. Chem. Soc.* **1990**, *112*, 5525–5534.

(33) All C–H bond lengths have been normalized to neutron-diffraction determined internuclear distance of 1.083 Å. See: (a) Steiner, T. *Angew. Chem., Int. Ed.* **2002**, *41*, 48–76. (b) Allen, F. H.; Kennard, O.; Watson, D. G.; Brammer, L.; Orpen, A. G.; Taylor, R. *J. Chem. Soc., Perkin Trans. 2* **1987**, S1–S19.

(34) (a) Nishio, M.; Hirota, M.; Umezawa, Y. *The CH/π Interaction: Evidence, Nature, and Consequences*, Wiley-VCH, New York, 1998. (b) Umezawa, Y.; Tsuboyama, S.; Honda, K.; Uzawa, J.; Nishio, M. *Bull. Chem. Soc. Jpn.* **1998**, *71*, 1207–1213. (c) Nishio, M.; Umezawa, Y.; Hirota, M.; Takeuchi, Y. *Tetrahedron* **1995**, *51*, 8665–8701.

(35) (a) Lee, W.-H.; Lee, H.; Kim, J.-A.; Choi, J.-H.; Cho, M.; Jeon, S.-J.; Cho, B. R. *J. Am. Chem. Soc.* **2001**, *123*, 10658–10667. (b) Zyss, J.; Ledoux, I. *Chem. Rev.* **1994**, *94*, 77–105.

(36) Heck, R. F. *Palladium Reagents in Organic Synthesis*; Academic Press: London/Orlando, 1985; pp 18.

(37) Leonard, K. A.; Nelen, M. I.; Anderson, L. T.; Gibson, S. L.; Hilf, R.; Detty, M. R. *J. Med. Chem.* **1999**, *42*, 3942–3952.

(38) Ziessel, R.; Suffert, J.; Youinou, M.-T. *J. Org. Chem.* **1996**, *61*, 6535–6546.